Table 3. Characteristics of Typical Target Cells for *in Vivo* Gene Transfer

Type of cell	Intestinal epithelial cells	Hepatocytes	Myotubes
Life span	<1 week	>5 months	Extremely long
Accessibility	Easy (Oral)	Difficult	Easy (Topical)
Blood flow[a]	Abundant (36 ml/h/g tissue)	Abundant (51 ml/h/g tissue)	Moderate (3 ml/h/g tissue)
Specific properties	Thick mucus layer	Specific receptors	Developed extracellular matrix

a) Values are calculated based on reported values.[115]

compared with viral promoters like CMV.

Lifespan of (Transfected) Cells If gene transfer occurs in differentiated cells, such as the lung epithelial or endothelial cells, hepatocytes, or skeletal myotubes, which is the most common for *in vivo* gene transfer by nonviral methods, the life-span of transfected cells limits sustained transgene expression. The lifespan of cells varies greatly depending on the type of cells: from less than 1 week for intestinal epithelial cells to life-long for nerve cells and skeletal and cardiac muscle cells. Table 3 compares the characteristics of potential target cells for *in vivo* gene transfer: intestinal epithelial cells, hepatocytes and myotubes.

Transgene expression in muscle cells can persist for several months after intramuscular injection,[116,117] indicating that a considerable fraction of the transfected cells survive for a long period. However, administration by this procedure may induce cell death. A large-volume injection of naked pDNA has resulted in an extremely high, but short, transgene expression,[92,93] and the procedure induced hepatocellular damage.[63] The loss of gene-expressing cells through an apoptotic process has been reported to occur in the lung following systemic administration of a cationic lipid–protamine–pDNA complex.[39]

NUMBER OF TRANSFECTED CELLS

As discussed in Table 1, the number of transfected cells is very important for cases in which transgene products localize within transfected cells *e.g.* dystrophin.[11] Although an intramuscular injection of naked pDNA results in relatively efficient transgene expression, transfected cells localize near the injection site and the efficiency is approximately 1% that of muscle fibers.[12,116] The disposition of transfected cells is limited to the region around the injection site, about 10 mm in diameter in dog muscle.[118] Direct injection into the liver also resulted in transgene expression over an area of 5 mm around the injection sites.[17] Limited disposition of pDNA injected locally is a major reason for this highly localized gene transfer (Fig. 4). When complexed with pDNA, cationic liposomes reduced the spread of pDNA in tumors following direct injection into the tissues.[44] Although the disposition of locally injected pDNA can be partially improved by using polyvinyl pyrrolidone,[119] hyaluronidase,[64,120] or electroporation,[90,121] these effects are limited to areas adjacent to the injection site.

Several approaches have been examined to overcome this hurdle. Injection of a sucrose solution prior to pDNA injection has been shown to force the generation of spaces between muscle fibers, thereby improving the disposition of pDNA throughout the muscle.[122] Digestion of extracellular matrix by proteases, such as collagenase and hyaluronidase, also increases gene transfer by naked pDNA or AAV vector,[64,120] and so could improve the disposition of those vectors within the muscle tissue injected. Molecules inducing muscle regeneration, such as bupivacaine, are also effective.[123,124]

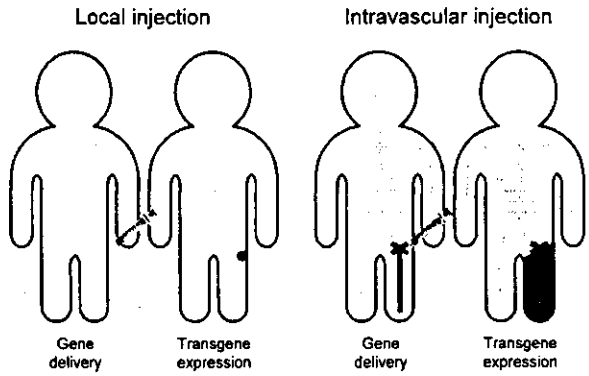

Fig. 4. Disposition and Gene Transfer of Locally or Intravascularly Injected pDNA

The disposition of pDNA injected into tissues is normally limited and, therefore, gene transfer will occur in cells very close to the injection site. On the other hand, intravascularly injected pDNA can distribute throughout tissues and have the opportunity to achieve gene transfer in a large number of cells. Pale lines represent blood vessels and solid areas represent cells expressing transgene products.

Another strategy for *in vivo* gene transfer to a large number of cells is intravascular delivery of pDNA. Due to the well-developed vasculature within tissues, such as internal organs, skeletal muscle and brain, pDNA can be delivered to the vicinity of a number of parenchymal cells of these tissues. Rapid injection of a large volume of naked pDNA solution resulted in very high transgene expression in the liver. Transfected cells were spread throughout the liver and approximately 40% of them expressed a transgene product.[92] A similar approach to skeletal muscle was also effective in inducing transgene expression in many myotubes in various species.[13–15] In monkeys, an average of 6.9% of myofibers were transfected in both leg and arm muscles.

Liu *et al.*[125] succeeded in gene transfer into the diaphragm muscle of the *mdx* mouse, a model of Duchenne muscular dystrophy (DMD). Significant gene transfer was also found after intravenous injection of naked pDNA followed by a brief occlusion of blood flow at the vena cava. Approximately 40% of muscle fibers of the diaphragm were positive for dystrophin in *mdx* mice injected with pDNA encoding the full-length *Dmd* cDNA.

CONCLUSION

Successful *in vivo* gene therapy requires the development of a rational gene transfer approach that fulfills various requirements for each target disease. Development of target cell-specific delivery and controlled release technologies, the combined use of a variety of approaches, and the optimization of administration methods are needed to achieve effective *in vivo* gene therapy. Further basic and clinical studies in this field should allow *in vivo* gene therapy to become a realistic medical option in the near future.

REFERENCES

1) Miao C. H., Thompson A. R., Loeb K., Ye X., *Mol. Ther.*, **3**, 947—957 (2001).
2) Fewell J. G., MacLaughlin F., Mehta V., Gondo M., Nicol F., Wilson E., Smith L. C., *Mol. Ther.*, **3**, 574—583 (2001).
3) Nishikawa M., Huang L., *Hum. Gene Ther.*, **12**, 861—870 (2001).
4) Nabel G. J., Nabel E. G., Yang Z. Y., Fox B. A., Plautz G. E., Gao X., Huang L., Shu S., Gordon D., Chang A. E., *Proc. Natl. Acad. Sci. U.S.A.*, **90**, 11307—11311 (1993).
5) Caplen N. J., Alton E. W., Middleton P. G., Dorin J. R., Stevenson B. J., Gao X., Durham S. R., Jeffery P. K., Hodson M. E., Coutelle C., Huang L., Porteous D. J., Williamson R., Geddes D. M., *Nat. Med.*, **1**, 39—46 (1995).
6) Snyder R. O., Miao C., Meuse L., Tubb J., Donahue B. A., Lin H. F., Stafford D. W., Patel S., Thompson A. R., Nichols T., Read M. S., Bellinger D. A., Brinkhous K. M., Kay M. A., *Nat. Med.*, **5**, 64—70 (1999).
7) Roth D. A., Tawa N. E., Jr., O'Brien J. M., Treco D. A., Selden R. F., *N. Engl. J. Med.*, **344**, 1735—1742 (2001).
8) Herzog R. W., Yang E. Y., Couto L. B., Hagstrom J. N., Elwell D., Fields P. A., Burton M., Bellinger D. A., Read M. S., Brinkhous K. M., Podsakoff G. M., Nichols T. C., Kurtzman G. J., High K. A., *Nat. Med.*, **5**, 56—63 (1999).
9) Kay M. A., Manno C. S., Ragni M. V., Larson P. J., Couto L. B., McClelland A., Glader B., Chew A. J., Tai S. J., Herzog R. W., Arruda V., Johnson F., Scallan C., Skarsgard E., Flake A. W., High K. A., *Nat. Genet.*, **24**, 257—261 (2000).
10) Kay M. A., High K., *Proc. Natl. Acad. Sci. U.S.A.*, **96**, 9973—9975 (1999).
11) Phelps S. F., Hauser M. A., Cole N. M., Rafael J. A., Hinkle R. T., Faulkner J. A., Chamberlain J. S., *Hum. Mol. Genet.*, **4**, 1251—1258 (1995).
12) Wolff J. A., Malone R. W., Williams P., Chong W., Acsadi G., Jani A., Felgner P. L., *Science*, **247**, 1465—1468 (1990).
13) Budker V., Zhang G., Danko I., Williams P., Wolff J. A., *Gene Ther.*, **5**, 272—276 (1998).
14) Liang K., Nishikawa M., Huang L., *Mol. Ther.*, **1**, S226 (2000).
15) Zhang G., Budker V., Williams P., Subbotin V., Wolff J. A., *Hum. Gene Ther.*, **12**, 427—438 (2001).
16) Lin H., Parmacek M. S., Morle G., Bolling S., Leiden J. M., *Circulation*, **82**, 2217—2221 (1990).
17) Hickman M. A., Malone R. W., Lehmann-Buinsma K., Sih T. R., Knoell D., Szoka F. C., Walzem R., Carlson D. M., Powell J. S., *Hum. Gene Ther.*, **5**, 1477—1483 (1994).
18) Budker V., Zhang G., Knechtle S., Wolff J. A., *Gene Ther.*, **3**, 593—598 (1996).
19) Wu G. Y., Wu C. H., *J. Biol. Chem.*, **263**, 14621—14624 (1991).
20) Perales J. C., Ferkol T., Beegen H., Ratnoff O. D., Hanson R. W., *Proc. Natl. Acad. Sci. U.S.A.*, **91**, 4086—4090 (1994).
21) Nishikawa M., Takemura S., Takakura Y., Hashida M., *J. Pharmacol. Exp. Ther.*, **287**, 408—415 (1998).
22) Nishikawa M., Takemura S., Yamashita F., Takakura Y., Meijer D. K., Hashida M., Swart P. J., *J. Drug Targeting*, **8**, 29—38 (2000).
23) Nishikawa M., Yamauchi M., Morimoto K., Ishida E., Takakura Y., Hashida M., *Gene Ther.*, **7**, 548—555 (2000).
24) Kawakami S., Fumoto S., Nishikawa M., Yamashita F., Hashida M., *Pharm. Res.*, **17**, 306—313 (2000).
25) Kawakami S., Sato A., Nishikawa M., Yamashita F., Hashida M., *Gene Ther.*, **7**, 292—299 (2001).
26) Ono T., Fujino Y., Tsuchiya T., Tsuda M., *Neurosci. Lett.*, **117**, 259—263 (1990).
27) Schwartz B., Benoist C., Abdallah B., Rangara R., Hassan A., Scherman D., Demeneix B. A., *Gene Ther.*, **3**, 405—411 (1996).
28) Raz E., Carson D. A., Parker S. E., Parr T. B., Abai A. M., Aichinger G., Gromkowski S. H., Singh M., Lew D., Yankauckas M. A., Baird A. M., Rhodes G. H., *Proc. Natl. Acad. Sci. U.S.A.*, **91**, 9519—9523 (1994).
29) Yoo J. J., Soker S., Lin L. F., Mehegan K., Guthrie P. D., Atala A., *J. Urol.*, **162**, 1115—1118 (1999).
30) Sikes M. L., O'malley B. W., Jr., Finegold M. J., Ledley F. D., *Hum. Gene Ther.*, **5**, 837—844 (1994).
31) Plautz G. E., Yang Z. Y., Wu B. Y., Gao Z., Huang L., Nabel G. J., *Proc. Natl. Acad. Sci. U.S.A.*, **90**, 4645—4649 (1993).
32) Son K., Huang L., *Gene Ther.*, **10**, 343—345 (1996).
33) Nomura T., Yasuda K., Yamada T., Okamoto S., Mahato R. I., Watanabe Y., Takakura Y., Hashida M., *Gene Ther.*, **6**, 121—129 (1999).
34) Kircheis R., Schuller S., Brunner S., Ogris M., Heider K. H., Zauner W., Wagner E., *J. Gene Med.*, **1**, 111—120 (1999).
35) Yoshimura K., Rosenfeld M. A., Nakamura H., Scherer E. M., Pavirani A., Lecocq J. P., Crystal R. G., *Nucleic Acids Res.*, **20**, 3233—3240 (1992).
36) McCluskie M. J., Chu Y., Xia J. L., Jessee J., Gebyehu G., Davis H. L., *Antisense Nucleic Acid Drug Devel.*, **8**, 401—414 (1998).
37) Ferkol T., Perales J. C., Eckman E., Kaetzel C. S., Hanson R. W., Davis P. B., *J. Clin. Invest.*, **95**, 493—502 (1995).
38) Liu Y., Mounkes L. C., Liggitt H. D., Brown C. S., Solodin I., Heath T. D., Debs R. J., *Nat. Biotechnol.*, **15**, 167—173 (1997).
39) Li S., Wu S. P., Whitmore M., Loeffert E. J., Wang L., Watkins S. C., Pitt B. R., Huang L., *Am. J. Physiol.*, **276**, L796—L804 (1999).
40) Sakurai F., Nishioka T., Saito H., Baba T., Okuda A., Matsumoto O., Taga T., Yamashita F., Takakura Y., Hashida M., *Gene Ther.*, **8**, 677—686 (2001).
41) Li S., Tan Y., Viroonchatapan E., Pitt B. R., Huang L., *Am. J. Physiol.*, **278**, L504—L511 (2000).
42) Hunt, C. A., MacGregor, R. D., Siegel, R. A., *Pharm. Res.*, **3**, 333—344 (1986).
43) Nara E., Masegi M., Hatono T., Hashida M., *Pharm. Res.*, **9**, 161—168 (1992).
44) Nomura T., Nakajima S., Kawabata K., Yamashita F., Takakura Y., Hashida M., *Cancer Res.*, **57**, 2681—2686 (1997).
45) Sandberg J. W., Lau C., Jacomino M., Finegold M., Henning S. J., *Hum. Gene Ther.*, **5**, 323—329 (1994).
46) Bennett H. S., Luft J. H., Hampton J. C., *Am. J. Physiol.*, **196**, 381—390 (1959).
47) Simionescu N., *Physiol. Rev.*, **63**, 1536—1579 (1983).
48) Ziylan Y. Z., Robinson P. J., Rapoport S. I., *Am. J. Physiol.*, **247**, R634—R638 (1984).
49) Rainov N. G., Ikeda K., Qureshi N. H., Grover S., Herrlinger U., Pechan P., Chiocca E. A., Breakefield X. O., Barnett F. H., *Hum. Gene Ther.*, **10**, 311—318 (1999).
50) Greelish J. P., Su L. T., Lankford E. B., Burkman J. M., Chen H., Konig S. K., Mercier I. M., Desjardins P. R., Mitchell M. A., Zheng X. G., Leferovich J., Gao G. P., Balice-Gordon R. J., Wilson J. M., Stedman H. H., *Nat. Med.*, **5**, 439—443 (1999).
51) Mahato R. I., Kawabata K., Takakura Y., Hashida M., *J. Drug Targeting*, **3**, 149—157 (1995).
52) Mahato R. I., Kawabata K., Nomura T., Takakura Y., Hashida M., *J. Pharm. Sci.*, **84**, 1267—1271 (1995).
53) Takakura Y., Takagi A., Hashida M., Sezaki H., *Pharm. Res.*, **4**: 293—300 (1987).
54) Takakura Y., Fujita T., Hashida M., Sezaki H., *Pharm. Res.*, **7**, 339—346 (1990).
55) Kawabata K., Takakura Y., Hashida M., *Pharm. Res.*, **12**, 825—830 (1995).
56) Yoshida M., Mahato R. I., Kawabata K., Takakura Y., Hashida M., *Pharm. Res.*, **13**, 599—603 (1996).
57) Takakura Y., Takagi T., Hashiguchi M., Nishikawa M., Yamashita F., Doi T., Imanishi T., Suzuki H., Kodama T., Hashida M., *Pharm. Res.*, **16**, 503—508 (1999).
58) Midoux P., Mendes C., Legrand A., Raimond J., Mayer R., Monsigny M., Roche A. C., *Nucl. Acids Res.*, **21**, 871—878 (1993).
59) Diebold S. S., Kursa M., Wagner E., Cotten M., Zenke M., *J. Biol. Chem.*, **274**, 19087—19094 (1999).
60) Wagner E., Zenke M., Cotten M., Beug H., Birnstiel M. L., *Proc. Natl. Acad. Sci. U.S.A.*, **87**, 3410—3414 (1990).
61) Ferkol T., Kaetzel C. S., Davis P. B., *J. Clin. Invest.*, **92**, 2394—2400 (1993).
62) Ross G. F., Morris R. E., Ciraolo G., Huelsman K., Bruno M., Whitsett J. A., Baatz J. E., Korfhagen T. R., *Hum. Gene Ther.*, **6**, 31—40 (1995).
63) Herweijer H., Zhang G., Subbotin V. M., Budker V., Williams P., Wolff J. A., *J. Gene Med.*, **3**, 280—291 (2001).
64) McMahon J. M., Signori E., Wells K. E., Fazio V. M., Wells D. J., *Gene Ther.*, **8**, 1264—1270 (2001).
65) Zhu X., Hadhazy M., Groh M. E., Wheeler M. T., Wollmann R., McNally E. M., *J. Biol. Chem.*, **276**, 21785—21790 (2001).

66) Capecchi M. R., *Cell*, **22**, 39—46 (1980).
67) Zabner J., Fasbender A. J., Moninger T., Poellinger K. A., Welsh M. J., *J. Biol. Chem.*, **270**, 18997—19007 (1995).
68) Lechardeur D., Sohn K. J., Haardt M., Joshi P. B., Monck M., Graham R. W., Beatty B., Squire J., O'brodovich H., Lukacs G. L., *Gene Ther.*, **6**, 482—497 (1999).
69) Kaneda Y., Iwai K., Uchida T., *J. Biol. Chem.*, **264**, 12126—12129 (1989).
70) Remy J.-S., Kichler A., Mordvinov V., Schuber F., Behr J.-P., *Proc. Natl. Acad. Sci. U.S.A.*, **92**, 1744—1748 (1995).
71) Zanta M. A., Belguise-Valladier P., Behr J.-P., *Proc. Natl. Acad. Sci. U.S.A.*, **96**, 91—96 (1999).
72) Plank C., Zauner W., Wagner E., *Adv. Drug Delivery Rev.*, **34**, 21—35 (1998).
73) Boussif O., Lezoualch F., Zanta M. A., Mergny M. D., Scherman D., Demeneix B., Behr J. P., *Proc. Natl. Acad. Sci. U.S.A.*, **92**, 7297—7301 (1995).
74) Midoux P., Monsigny M., *Bioconjugate Chem.*, **10**, 406—441 (1999).
75) Benns J. M., Choi J. S., Mahato R. I., Park J. S., Kim S. W., *Bioconjugate Chem.*, **11**, 637—645 (2000).
76) Putnam D., Gentry C. A., Pack D. W., Langer R., *Proc. Natl. Acad. Sci. U.S.A.*, **98**, 1200—1205 (2001).
77) Xu Y., Szoka F. C., Jr., *Biochemistry*, **35**, 5616—5623 (1996).
78) Sakurai F., Inoue R., Nishino Y., Okuda A., Matsumoto O., Taga T., Yamashita F., Takakura Y., Hashida M., *J. Controlled Release*, **66**, 255—269 (2000).
79) Yang N. S., Burkholder J., Roberts B., Martinell B., McCabe D., *Proc. Natl. Acad. Sci. U.S.A.*, **87**, 9568—9572 (1990).
80) Williams R. S., Johnston S. A., Riedy M., Devit M. J., Mcelligott S. G., Sanford J. C., *Proc. Natl. Acad. Sci. U.S.A.*, **88**, 2726—2730 (1991).
81) Zelenin A. V., Kolesnikov V. A., Tarasenko O. A., Shafei R. A., Zelenina I. A., Mikhailov V. V., Semenova M. L., Kovalenko D. V., Artemyeva O. V., Ivaschnko T. E., Evgrafov O. V., Dickson G., Baranovand V. S., *FEBS Lett.*, **414**, 319—322 (1997).
82) Furth P. A., Shamay A., Wall R. J., Henninghausen L., *Anal. Biochem.*, **205**, 365—368 (1992).
83) Walther W., Stein U., Fichtner I., Malcherek L., Lemm M., Schlag P. M., *Gene Ther.*, **8**, 173—180 (2001).
84) Mir L. M., Banoun H., Paoletti C., *Exp. Cell Res.*, **175**, 15—25 (1988).
85) Somiari S., Glasspool-Malone J., Drabick J. J., Gilbert R. A., Heller R., Jaroszeski M. J., Malone R. W., *Mol. Ther.*, **2**, 178—187 (2000).
86) Johnson P. G., Gallo S. A., Hui S. W., Oseroff A. R., *J. Invest. Dermatol.*, **111**, 457—463 (1998).
87) Titomirov A. V., Sukharev S., Kistanova E., *Biochim. Biophys. Acta*, **1088**, 131—134 (1991).
88) Heller R., Jaroszeski M., Atkin A., Moradpour D., Gilbert R., Wands J., Nicolau C., *FEBS Lett.*, **389**, 225—228 (1996).
89) Rols M. P., Delteil C., Golzio M., Dumond P., Cros S., Teissie J., *Nat. Biotechnol.*, **16**, 168—171 (1998).
90) Aihara H., Miyazaki J., *Nat. Biotechnol.*, **16**, 867—870 (1998).
91) Huber P. E., Pfisterer P., *Gene Ther.*, **7**, 1516—1525 (2000).
92) Liu F., Song Y. K., Liu D., *Gene Ther.*, **6**, 1258—1266 (1999).
93) Zhang G., Budker V., Wolff J. A., *Hum. Gene Ther.*, **10**, 1735—1737 (1999).
94) Kobayashi N., Kuramoto T., Yamaoka K., Hashida M., Takakura Y., *J. Pharmacol. Exp. Ther.*, **297**, 853—860 (2001).
95) Xu Z. L., Mizuguchi H., Ishii-Watabe A., Uchida E., Mayumi T., Hayakawa T., *Gene*, **272**, 149—156 (2001).
96) Truong-Le V. L., August J. T., Leong K. W., *Hum. Gene Ther.*, **9**, 1709—1717 (1998).
97) Ochiya T., Takahama Y., Nagahara S., Sumita Y., Hisada A., Itoh H., Nagai Y., Terada M., *Nat. Med.*, **5**, 707—710 (1999).
98) Capan Y., Woo B. H., Gebrekidan S., Ahmed S., DeLuca P. P., *Pharm. Res.*, **16**, 509—513 (1999).
99) Klugherz B. D., Jones P. L., Cui X., Chen W., Meneveau N. F., DeFelice S., Connolly J., Wilensky R. L., Levy R. J., *Nat. Biotechnol.*, **18**, 1181—1184 (2000).
100) Guo Z. S., Wang L. H., Eisensmith R. C., Woo S. L. C., *Gene Ther.*, **3**, 802—810 (1996).
101) Bird A. P., *Trends Genet.*, **3**, 342—347 (1987).
102) Krieg A. M., Yi A. K., Matson S., Waldschmidt T. J., Bishop G. A., Teasdale R., Koretzky G. A., Klinman D. M., *Nature* (London), **374**, 546—549 (1995).
103) Paillard F., *Hum. Gene Ther.*, **10**, 2089—2090 (1999).
104) Krieg A. M., Wu T., Weeratna R., Efler S. M., Love-Homan L., Yang L., Yi A.-K., Short D., Davis H. L., *Proc. Natl. Acad. Sci. U.S.A.*, **95**, 12631—12636 (1998).
105) McMahon J. M., Wells K. E., Bamfo J. E., Cartwright M. A., Wells D. J., *Gene Ther.*, **5**, 1283—1290 (1998).
106) Yew N. S., Wang K. X., Przybylaka M., Bagley R. G., Stedman M., Marshall J., Scheule R. K., Cheng S. H., *Hum. Gene Ther.*, **10**, 223—234 (1999).
107) Tousignant J. D., Gates A. L., Ingram L. A., Johnson C. L., Nietupski J. B., Cheng S. H., Eastman S. J., Scheule R. K., *Hum. Gene Ther.*, **11**, 2493—2513 (2000).
108) Yew N. S., Zhao H., Wu I.-H., Song A., Tousignant J. D., Przybylska M., Cheng S. H., *Mol. Ther.*, **1**, 255—262 (2000).
109) Tan Y., Li S., Pitt B. R., Huang L., *Hum. Gene Ther.*, **10**, 2153—2161 (1999).
110) Hofman C. R., Dileo J. P., Li Z., Li S., Huang L., *Gene Ther.*, **8**, 71—74 (2001).
111) Yew N. S., Wysokenski D. M., Wang K. X., Ziegler R. J., Marshall J., McNeilly D., Cherry M., Osburn W., Cheng S. H., *Hum. Gene Ther.*, **8**, 575—584 (1997).
112) Loser P., Jennings G. S., Strauss M., Sandig V., *J. Virol.*, **72**, 180—190 (1998).
113) Qin L., Ding Y., Pahud D. R., Chang E., Imperiale M. J., Bromberg J. S., *Hum. Gene Ther.*, **8**, 2019—2029 (1997).
114) Yew N. S., Przybylska M., Ziegler R. J., Liu D., Cheng S. H., *Mol. Ther.*, **4**, 75—82 (2001).
115) Bischoff K. B., Dedrick R. L., Zaharko D. S., Longstreth J. A., *J. Pharm. Sci.*, **60**, 1128—1133 (1971).
116) Acsadi G., Dickson G., Love D. R., Jani A., Walsh F. S., Gurusinghe A., Wolff J. A., Davies K. E., *Nature* (London), **352**, 815—818 (1991).
117) Manthorpe M., Cornefert-Jensen F., Hartikka J., Felgner J., Rundell A., Margalith M., Dwarki V., *Hum. Gene Ther.*, **4**, 419—431 (1993).
118) O'hara A. J., Howell J. M., Taplin R. H., Fletcher S., Lloyd F., Kakulas B., Lochmuller H., Karpati G., *Muscle Nerve*, **24**, 488—495 (2001).
119) Mumper R. J., Duguid J. G., Anwer K., Barron M. K., Nitta H., Rolland A. P., *Pharm. Res.*, **13**, 701—709 (1996).
120) Favre D., Cherel Y., Provost N., Blouin V., Ferry N., Moullier P., Salvetti A., *Gene Ther.*, **7**, 1417—1420 (2000).
121) Mathiesen I., *Gene Ther.*, **6**, 508—514 (1999).
122) Davies H. L., Whalen R. G., Demeneix B. A., *Hum. Gene Ther.*, **4**, 151—159 (1993).
123) Wells D. J., *FEBS Lett.*, **332**, 179—182 (1993).
124) Danko I., Fritz J. D., Jiao S., Hogan K., Latendresse J. S., Wolff J. A., *Gene Ther.*, **1**, 114—121 (1994).
125) Liu F., Nishikawa M., Clemens P. R., Huang L., *Mol. Ther.*, **4**, 45—51 (2001).

Int. J. Cancer: **99**, 474–479 (2002)

Publication of the International Union Against Cancer

INHIBITION OF EXPERIMENTAL PULMONARY METASTASIS BY CONTROLLING BIODISTRIBUTION OF CATALASE IN MICE

Makiya NISHIKAWA, Ayumi TAMADA, Hitomi KUMAI, Fumiyoshi YAMASHITA and Mitsuru HASHIDA*

Department of Drug Delivery Research, Graduate School of Pharmaceutical Sciences, Kyoto University, Kyoto, Japan

In a previous study, we showed that targeted delivery of bovine liver catalase to hepatocytes by direct galactosylation augmented the inhibitory effect of the enzyme on experimental hepatic metastasis of colon carcinoma cells (unpublished data). Here, we examined the ability of catalase to inhibit tumor metastasis to the lung by controlling its biodistribution. Four types of catalase derivative, Gal-CAT, Man-CAT, Suc-CAT and PEG-CAT, were synthesized. Experimental pulmonary metastasis was induced in mice by i.v. injection of 1×10^5 colon 26 tumor cells. An i.v. injection of catalase (35,000 units/kg) partially, but significantly, decreased the number of colonies in the lung 2 weeks after tumor injection, from 93 ± 29 (saline injection) to 63 ± 23 ($p < 0.01$). Suc-CAT, Man-CAT and Gal-CAT showed effects similar to those of catalase on the number of colonies. However, PEG-CAT greatly inhibited pulmonary metastasis to 22 ± 11 ($p < 0.001$). Furthermore, s.c. injection of catalase also greatly inhibited metastasis (11 ± 6, $p < 0.001$). Neither inactivated catalase nor BSA showed any effects on the number of metastatic colonies, indicating that the enzymatic activity of catalase to detoxify H_2O_2 is the critical factor inhibiting metastasis. ^{111}In-PEG-CAT showed a sustained concentration in plasma, whereas s.c.-injected ^{111}In-catalase was slowly absorbed from the injection site. These results suggest that retention of catalase activity in the circulation is a promising approach to inhibit pulmonary metastasis.

Key words: *catalase; metastasis; reactive oxygen species; chemical modification; colon carcinoma*

Metastasis is the leading cause of death from cancer. It can be roughly divided into the following steps: tumor cell dissociation, invasion, intravasation, distribution to distant organs, arrest in small vessels, adhesion to endothelial cells, extravasation, invasion into the target organ and proliferation.[1] ROS regulate the expression levels of molecules involved in the above processes of metastasis. For example, ROS are involved in the regulation of the expression levels of adhesion molecules[2,3] and proteases such as MMPs.[4–6] In addition, low-level ROS, especially H_2O_2, increase cell proliferation.[7,8]

Several studies have shown that removal of ROS by antioxidant enzymes such as catalase and SOD can inhibit the incidence of tumor metastasis in various animal models.[9–11] These enzymes, however, have unique biodistribution characteristics depending on their physicochemical properties; catalase is cleared by hepatocytes, whereas SOD is filtered at the kidney.[12,13] Therefore, to show their pharmacologic effects on tumor metastasis, their biodistribution should be controlled by any means corresponding to the tissue disposition of metastasizing tumor cells. In a previous study, we inhibited experimental hepatic metastasis of colon carcinoma cells in mice by synthesizing hepatocyte-targetable Gal-CAT (unpublished data). These results indicate the importance of targeted delivery of antioxidant enzymes to sites where tumor cells are going to metastasize.

Because the lung is the first organ encountered by tumor cells detached from primary tumors in most cases, it is a major site for tumor metastasis. The continuous capillary endothelium of the lung as well as the basement membrane restrict the entry of tumor cells into the tissue parenchyma. Therefore, tumor cells must destroy these barriers to form metastatic colonies in the organ. Targeting of catalase to the lung or prolongation of its concentration in plasma would be good approaches to inhibit pulmonary metastasis.

In the present study, experimental pulmonary metastasis was induced in mice by i.v. injection of colon 26 mouse colon carcinoma cells. The tissue distribution of tumor cells was studied following i.v. injection of ^{111}In-labeled cells. Various catalase derivatives were administered by i.v. or s.c. injection to mice inoculated with tumor cells. The effects of catalase derivatives were examined by measuring the number of metastatic colonies in the lung. Tumor cells pretreated with catalase or H_2O_2 were also injected into mice, to examine the direct effects of these reagents on the metastatic ability of the tumor cells.

MATERIAL AND METHODS

Animals

BALB/c (4 weeks old, male), CDF_1 (6 weeks old, male) and ddY (6 weeks old, male) mice were purchased from the Shizuoka Agricultural Cooperative Association for Laboratory Animals (Shizuoka, Japan). Animals were maintained under conventional housing conditions. All animal experiments were carried out in accordance with the guidelines for animal experiments of Kyoto University.

Chemicals

Bovine liver catalase (C-100, 35,000 units/mg) was purchased from Sigma (St. Louis, MO). [^{111}In]Cl_3 was supplied by Nihon Medi-Physics (Takarazuka, Japan). Catalase derivatives Suc-CAT, Man-CAT, Gal-CAT and PEG-CAT as well as inactivated catalase were synthesized as reported previously.[14] The remaining enzymatic activity of the catalase derivatives was determined to be 86%, 90%, 97% and 96% of the original activity for Suc-CAT, Gal-CAT, Man-CAT and PEG-CAT, respectively. All other chemicals were of the highest grade available.

Tumor cells

Colon 26 tumor cells, obtained from Dr. T. Yamori (Cancer Chemotherapeutic Center of the Cancer Institute, Tokyo, Japan), were maintained *in vivo* by s.c. transplantation into BALB/c mice.

Abbreviations: Gal-CAT, galactosylated catalase; Man-CAT, mannosylated catalase; MMP, matrix metalloproteinase; PEG-CAT, polyethylene glycol–conjugated catalase; ROS, reactive oxygen species; SOD, superoxide dismutase; Suc-CAT, succinylated catalase.

Grant sponsor: Ministry of Education, Science, Sports and Culture of Japan.

*Correspondence to: Department of Drug Delivery Research, Graduate School of Pharmaceutical Sciences, Kyoto University, Sakyo-ku, Kyoto 606-8501, Japan. Fax: +81-75-753-4575.
E-mail: hashidam@pharm.kyoto-u.ac.jp

Received 19 September 2001; Revised 2 January 2002; Accepted 8 February 2002

DOI 10.1002/ijc.10387
Published online 26 March 2002 in Wiley InterScience (www.interscience.wiley.com).

For experimental pulmonary metastasis studies, tumor tissue was excised from mice and minced into small pieces in HBSS on ice. After treatment with trypsin, colon 26 cells were passed through a filter and washed with PBS (pH 7.4); the cell concentration was adjusted to 10^6 cells/ml in HBSS. For tissue distribution experiments on tumor cells in mice, colon 26 cells were radiolabeled using ^{111}In-oxine, according to the method of Thakur *et al.*[15]

Biodistribution of colon 26 tumor cells in mice

^{111}In-labeled colon 26 cells (1×10^5 cells/100 μl HBSS) were injected into a tail vein. At 1, 8 and 24 hr after injection, blood was collected from the vena cava under ether anesthesia and mice were killed. The liver, kidney, spleen, lung and heart were removed and rinsed with saline. Radioactivity in tissue samples was counted with a well-type NaI-scintillation counter (ARC-500; Aloka, Tokyo, Japan).

Experimental pulmonary metastasis

Experimental pulmonary metastasis was induced by injecting 1×10^5 colon 26 tumor cells in 0.1 ml HBSS into a tail vein of CDF_1 mice. One hour after tumor injection, catalase or its derivative was injected i.v. or s.c. at a dose of 35,000 units/kg (approx. 1 mg/kg for unmodified catalase). Two weeks after tumor inoculation, the lung was excised, weighed and fixed with methanol; then, pulmonary metastatic colonies was counted. To examine the effects of pretreatment of catalase and H_2O_2 on tumor metastasis, colon 26 cells exposed to various concentrations of catalase or H_2O_2 for 16 hr were also used in the metastasis experiments as above.

Biodistribution of ^{111}in-catalase derivatives

Catalase derivatives were radiolabeled with ^{111}In as reported previously.[14] The solution of ^{111}In-catalase derivative was injected i.v. or s.c. in male ddY mice at a dose of 1 mg/kg. At appropriate intervals after injection, blood was collected from the vena cava under ether anesthesia and mice were killed. Then, plasma was obtained by centrifugation of the blood collected. The lung, liver, kidney and spleen were removed, rinsed with saline and weighed. In cases with s.c. injection, the skin and underlying muscle around the injection site were also collected as a sample of the injection site. The brachial lymph nodes were collected as a major route of drainage from the injection site. Radioactivity was counted with the well-type NaI-scintillation counter.

Measurement of catalase activity in mouse tissues

Experimental pulmonary metastasis was induced by injecting colon 26 tumor cells into BALB/c mice as above. Two weeks after tumor inoculation, mice were killed and 200 μl blood were collected from the vena cava with a heparinized syringe. Erythrocytes separated by centrifugation were washed with saline and lysed with water. The liver and lung were perfused with saline to remove erythrocytes as much as possible, then excised, weighed and homogenized with a lysis buffer [0.05% Triton X-100, 2 mM EDTA, 0.1 M TRIS (pH 7.8)]. Catalase activity in the lysed erythrocytes and the supernatant of tissue homogenates was measured as previously reported.[14]

Statistical analysis

Differences were statistically evaluated by 1-way ANOVA, followed by the Student-Newmann-Keuls multiple-comparison test. Two-column comparisons were analyzed using Student's *t*-test.

RESULTS

Biodistribution of colon 26 tumor cells

Figure 1 shows the radioactivity in tissue samples of mice injected with ^{111}In-colon 26 tumor cells into a tail vein at 1, 8 and 24 hr after injection. Approximately 8% of the injected radioactivity was detected in the lung at 1 hr, and the radioactivity decreased with time to 1.2% at 24 hr. More radioactivity was

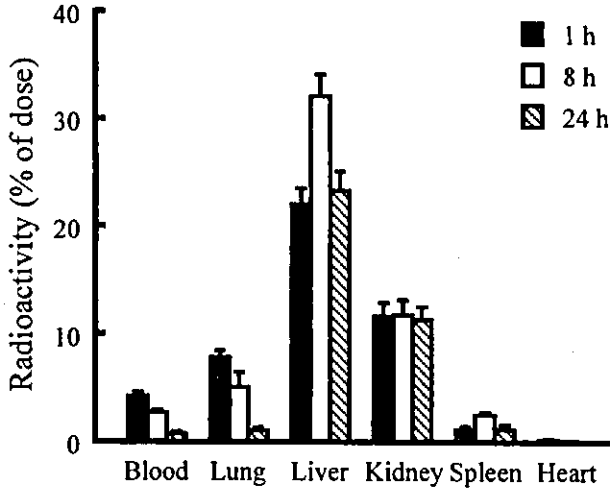

FIGURE 1 – Tissue distribution of radioactivity in mice following i.v. injection of ^{111}In-colon 26 tumor cells. Results are expressed as means ± SD of 3 mice.

detected in the liver (22–32% of dose) and the kidney (12%). Although these organs had more radioactivity than the lung, metastatic colonies were detected only in the lung. The biodistribution of the radioactivity following intraportal injection of ^{111}In-colon 26 tumor cells was different from that following i.v. injection (unpublished data), suggesting that the biodistribution of tumor cells and the formation of metastatic colonies depend on the administration route. Administration of catalase (1 mg/kg) by i.v. or s.c. injection hardly altered the biodistribution profiles of radioactivity following injection of ^{111}In-colon 26 tumor cells (data not shown).

Effect of pretreatment of colon 26 cells with catalase or H_2O_2 on metastasis

Colon 26 tumor cells were incubated *in vitro* with saline (control), catalase (500 or 1,000 units/ml), H_2O_2 (1, 2 or 4 μM), inactivated catalase (an equivalent concentration to 500 units catalase/ml) or BSA. Then, tumor cells (1×10^5) were injected into a tail vein of mice and metastatic colonies in the lung counted at 2 weeks. Injection of saline-treated tumor cells resulted in the formation of 130 ± 43 colonies/mouse lung (Fig. 2). Cells pretreated with catalase decreased the number of lung colonies (104 ± 16 for 500 units/ml and 101 ± 8 for 1,000 units/ml). However, treatment with H_2O_2 increased the number of colonies in a H_2O_2 concentration-dependent manner. Neither inactivated catalase nor BSA showed any effects on the number of metastases. The numbers of lung colonies with H_2O_2-pretreated cells were significantly greater than those with catalase-pretreated cells ($p < 0.01$).

Pulmonary metastasis and its inhibition by catalase derivatives

Figure 3 shows typical tissue images of the mouse lung with tumor colonies. The number of metastatic colonies was 93 ± 29 for the saline (vehicle)-treatment group at 2 weeks after injection of 1×10^5 cells (Fig. 4).

An i.v. injection of catalase at a dose of 35,000 units/kg (1 mg/kg) significantly reduced the number of metastatic colonies in the lung to 63 ± 23 ($p < 0.01$, Figs. 3, 4). The numbers of colonies in mice treated with Suc-CAT, Man-CAT or Gal-CAT were almost identical to the numbers in the catalase-treatment group ($p < 0.01$ against the saline-treatment group). However, PEG-CAT showed an inhibitory effect on the number of colonies in the lung greater than the other catalase derivatives; only 22 ± 11 colonies were counted 2 weeks after tumor inoculation ($p < 0.001$ against the saline-treatment group). Furthermore, s.c. injection of catalase also greatly prevented metastasis (11 ± 6, $p < 0.001$ against the

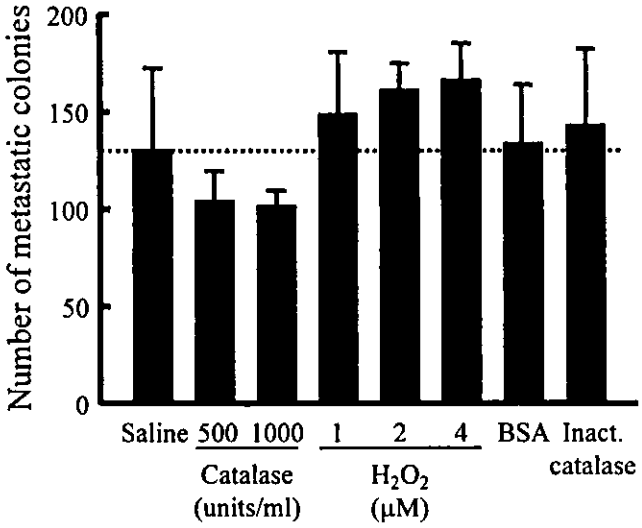

FIGURE 2 – Number of metastatic colonies of colon 26 tumor cells in the lung of mice injected with colon 26 tumor cells. Tumor cells (1×10^5/mouse) pretreated with saline (vehicle), catalase (500 or 1,000 units/ml), H_2O_2 (1, 2 or 4 μM), BSA or inactivated catalase for 16 hr *in vitro* were injected into mice through a tail vein. Then, mice were killed 14 days after tumor injection, and the number of colonies was determined. Results are expressed as means ± SD of at least 4 mice. Numbers of colonies with H_2O_2-pretreated cells were significantly different from those with catalase-pretreated cells ($p < 0.01$).

saline-treatment group). The inhibitory effects of PEG-CAT and s.c. catalase on metastasis were significantly greater than the effect of i.v. catalase ($p < 0.01$). Neither inactivated catalase nor BSA showed any effects on the number of metastases, indicating that the enzymatic activity of catalase to detoxify H_2O_2 is the critical factor preventing metastasis.

Biodistribution of ^{111}In-catalase derivatives

Figure 5 shows the amount in the lung and concentration in plasma of ^{111}In-catalase derivatives in mice following i.v. injection at a dose of 1 mg/kg. No ^{111}In-catalase derivative showed a pronounced accumulation in the lung (<1% of dose) 1 hr after injection. The concentration in plasma, however, largely differed among the derivatives in the following order: ^{111}In-PEG-CAT > ^{111}In-catalase > other ^{111}In-catalase derivatives.

The time courses of the biodistribution of ^{111}In-catalase and ^{111}In-PEG-CAT were then examined after i.v. or s.c. injection (Fig. 6). ^{111}In-catalase injected i.v. rapidly disappeared from the plasma and accumulated in the liver, whereas ^{111}In-PEG-CAT exhibited prolonged retention in the plasma and slowly accumulated in various organs. When injected s.c., ^{111}In-catalase remained at the injection site for a long time and slowly disappeared with half-life of approximately 27 hr.

Catalase activity in mouse tissues

Table I summarizes the catalase activity in mouse tissues. In normal mice, the greatest amount of catalase activity was contained in the liver, followed by erythrocytes and the lung. Catalase activity in the liver and erythrocytes was not changed by the presence of tumor colonies in the lung. However, catalase activity in the lung of mice with pulmonary colonies was significantly lower than that in control mice. Figure 7 shows the relation of catalase activity (units/g tissue) and lung weight. Increasing tissue weight due to growth of tumor colonies decreased catalase activity, indicating that tumor tissue has less catalase activity than lung tissue.

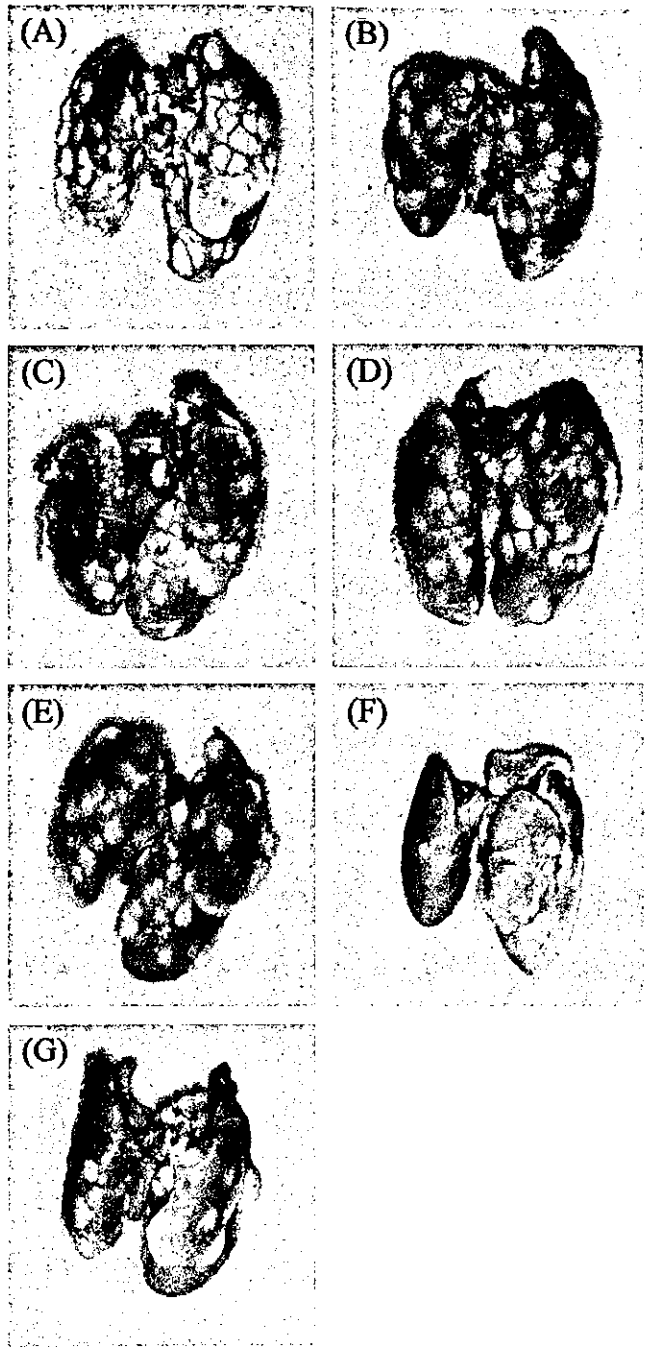

FIGURE 3 – Typical examples of pulmonary metastases in mice receiving i.v. injection of 1×10^5 colon 26 tumor cells followed by injection of a catalase derivative. *(a)* saline (vehicle), *(b)* catalase (i.v.), *(c)* Suc-CAT, *(d)* Man-CAT, *(e)* Gal-CAT, *(f)* PEG-CAT and *(g)* catalase (s.c.). Each catalase derivative was injected at a dose of 35,000 units/kg 1 hr after tumor inoculation.

DISCUSSION

Because of the complexity and multiple-step nature of tumor metastasis, antimetastatic strategies include diverse approaches: surgical resection, radiation, immunotherapy, chemotherapy and administration of angiogenic or protease inhibitors. However, some of these approaches are not suitable for antimetastatic therapy because of their localized effects and/or severe side effects.

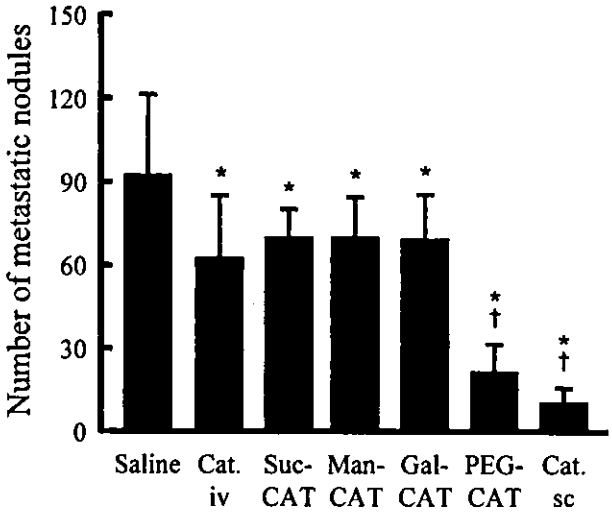

FIGURE 4 – Number of metastatic colonies of colon 26 tumor cells in the lung of mice injected with saline (vehicle) or catalase derivative (35,000 units/kg). Mice were killed 14 days after tumor injection, and the number of colonies was determined. Results are expressed as means ± SD of at least 6 mice. *Statistically significant difference compared to the saline group ($p < 0.01$). †Statistically significant difference compared to the catalase (i.v.) group ($p < 0.01$).

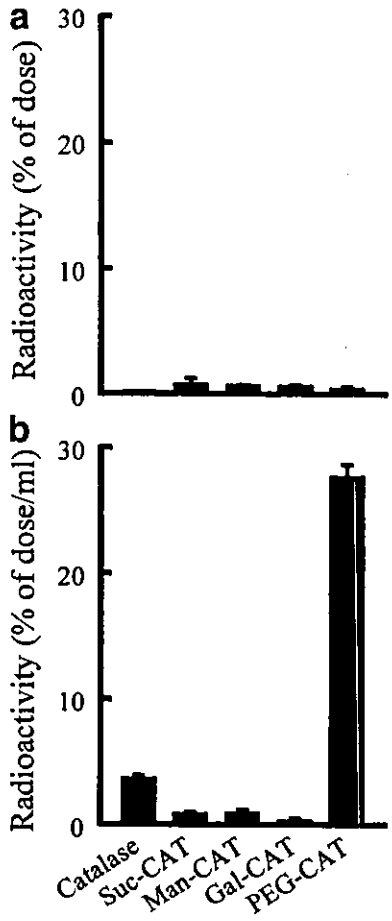

FIGURE 5 – Tissue distribution of ^{111}In-catalase derivatives following i.v. injection in mice at a dose of 1 mg/kg. *(a)* Amount of radioactivity accumulated in the lung at 1 hr. *(b)* Concentration of radioactivity in plasma at 1 hr. Results are expressed as means ± SD of 3 mice.

Antimetastatic therapy should possess long-lasting and systemic effects as well as low toxicity.

ROS are involved in various aspects of tumor metastasis;[2-8] therefore, their removal can be a promising approach in antimetastatic therapy of tumor. To this end, antioxidant enzymes such as catalase and SOD have been used in animal models and found to be effective at inhibiting tumor metastasis.[9-11] Although these studies showed the usefulness of these enzymes as reagents for antimetastatic therapy, they would be effective only when delivered to the site of metastasis of tumor cells, where ROS are produced and facilitate tumor metastasis.

The biodistribution of tumor cells, therefore, is an important factor in designing a strategy of targeted delivery of antioxidant enzymes for inhibition of tumor metastasis. The radioactivity following i.v. injection of ^{111}In-colon 26 tumor cells was distributed to various organs, including the liver, kidney, lung and spleen (Fig. 1). Although the radioactivity data showed that the liver was the major organ for uptake, metastatic colonies of tumor cells were detected only in the lung following i.v. injection of colon 26 tumor cells. Most tumor cells die within the blood circulation following intravascular injection, and fewer than 0.05% survive to form metastasis.[16] When ^{111}In-colon 26 tumor cells were injected intraportally, the radioactivity extensively (>50% of dose) accumulated and metastatic colonies formed only in the liver (unpublished data). These results indicate that, in experimental tumor metastasis models, the target organ for metastasis is strictly dependent on the route of injection of tumor cells and that, when injected i.v., the lung is the only target organ for tumor metastasis. The biodistribution of radioactivity following injection of ^{111}In-colon 26 tumor cells was hardly affected by administration of catalase i.v. or s.c., under conditions where it effectively inhibited tumor metastasis. These results suggest that the early steps of metastasis, including the physical entrapment of tumor cells in capillaries,[17] are hardly influenced by catalase. Therefore, the inhibitory effects of catalase should be related to the later steps of metastasis.

After adsorption to the surface of endothelial cells, tumor cells need to extravasate to form metastatic colonies at the site. Then, they require proteases that digest the basement membranes and the extracellular matrix, which act as physical barriers to tumor cells metastasizing into tissue parenchyma. MMPs are the major proteolytic enzymes involved in the invasion of tumor cells.[18] In metastatic foci, MMPs are produced by both tumor cells and host cells, such as infiltrating macrophages. Colon 26 tumor cells expressed some MMPs *in vitro*, and their activities in the medium were enhanced by sublethal H_2O_2 but diminished by catalase (unpublished data). Injection of colon 26 tumor cells treated with catalase *in vitro* resulted in a decreased number of metastatic colonies in the lung, suggesting that catalase can directly reduce the metastatic ability of tumor cells, probably through reduction of MMPs.[4,5] Increased numbers of colonies with tumor cells treated with H_2O_2 also supports the inhibitory effect of catalase on the invasive ability of the cells. A high H_2O_2 concentration is cytotoxic to various cells, including tumor cells. Yang *et al.*[19] reported that 80 μM H_2O_2 is the IC_{50} for a human T-lymphoblastic leukemia cell. However, without any obvious cytotoxicity, low H_2O_2 concentrations (several micromolar or less, depending on the cell type) can induce various changes in cells, including increased gelatinase activity[20] and proliferation.[8] Some tumor cells produce large amounts of H_2O_2.[6,21] When incubated with low H_2O_2 concentrations *in vitro*, therefore, the cellular activities in proteolytic enzymes and/or proliferation could increase, resulting in increased numbers of colonies in mice injected with H_2O_2-pretreated tumor cells. Furthermore, extracellularly added catalase is reported to decrease cellular activities enhanced by the presence of H_2O_2,[8,21] supporting fewer pulmonary colonies in mice injected with catalase-treated colon 26 tumor cells.

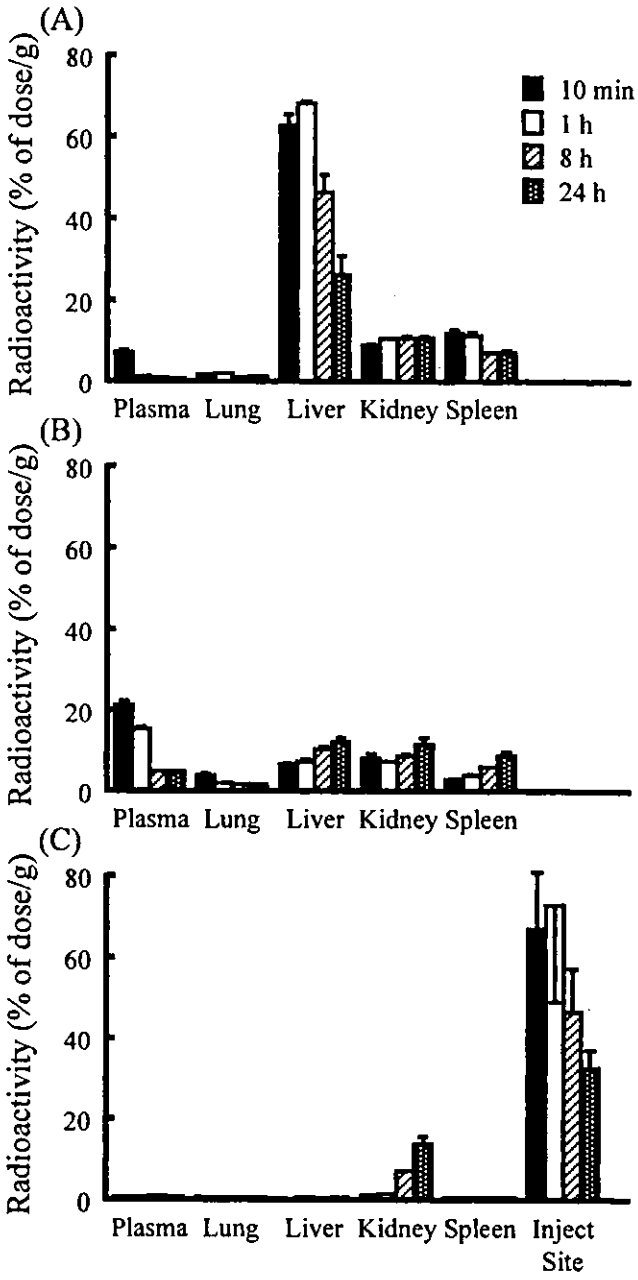

FIGURE 6 – Tissue distribution of ^{111}In-catalase derivatives in mice injected at a dose of 1 mg/kg. (a) ^{111}In-catalase following i.v. injection. *(b)* ^{111}In-PEG-CAT following i.v. injection. *(c)* ^{111}In-catalase following s.c. injection. Results are expressed as means ± SD of 3 mice.

In a different experiment (unpublished data), we examined the antimetastatic effects of catalase derivatives in mice with experimental hepatic metastasis. Gal-CAT, which is most effectively delivered to hepatocytes *via* asialoglycoprotein receptor–mediated uptake,[14] showed the greatest inhibitory effect on the experimental hepatic metastasis of colon 26 tumor cells compared to other catalase derivatives. These results clearly indicate that targeting of catalase is important for its application to antimetastatic therapy. When tumor cells metastasize to other organs, therefore, another strategy for delivery of catalase should be required. Bovine liver catalase has affinity with hepatocytes and, following i.v. injection, rapidly disappears from the systemic circulation and is delivered to hepatocytes.[13] Suc-, Man- and Gal-CAT are also rapidly delivered to the liver *via* scavenger, mannose and asialoglycoprotein receptor–mediated processes, respectively.[14] These 4 catalase derivatives showed significant but marginal effects, decreasing the number of metastatic colonies in the lung. However, PEG-CAT, a long-circulating derivative of catalase, showed a marked reduction of metastatic colonies in the lung. The major difference between PEG-CAT and the others is its biodistribution profile following i.v. injection (Fig. 5). Like other PEG-conjugated proteins, PEG-CAT had a longer plasma half-life and was slowly delivered to various organs, including the lung. This prolonged circulation of PEG-CAT would be the reason for its greater potential to inhibit metastasis compared to the other derivatives. All catalase derivatives showed marked accumulation in the lung.

TABLE I – CATALASE ACTIVITY IN TISSUES OF BALB/C MICE

Tissue	Catalase activity (units/g tissue or units/ml blood)	
	Without metastatic colonies	With metastatic colonies
Lung	2,390 ± 160	1,430 ± 360[1]
Liver	66,100 ± 19,300	69,400 ± 10,400
Erythrocytes	6,340 ± 1,930	4,920 ± 900

[1]Statistically significant difference ($p < 0.01$) from the activity in mice without metastatic colonies in the lung.

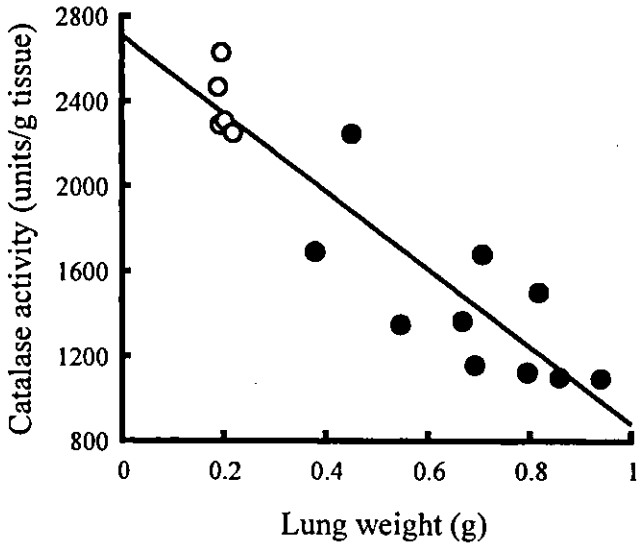

FIGURE 7 – Catalase activity in the lung of mice. Open circles, control mice (without metastatic colonies); solid circles, mice with pulmonary metastatic colonies of colon 26 tumor cells.

The biodistribution of drugs, including proteins such as catalase, depends on the administration route. Because of absorption from the injection site into the blood, s.c.-injected compounds show prolonged profiles of concentration in plasma. When ^{111}In-catalase was s.c.-injected, it disappeared very slowly from the injection site, with an apparent half-life of 27 hr (Fig. 5). Although the concentration in plasma was very low (<1% of dose/ml) and the amount delivered to the lung was minimal throughout the experimental period of 24 hr, s.c.-injected catalase showed the greatest effect on the inhibition of pulmonary metastasis. Chang and Poznansky[22] reported that i.p. injection of microcapsules containing catalase efficiently decomposed s.c.-injected sodium perborate in acatalasemic mice, which have very reduced blood and total catalase activities. Here, we show that catalase injected s.c. might detoxify H_2O_2 and decrease the level of systemic oxidants without entering the blood circulation. Such a possibility should be investigated in future experiments. However, in normal mice, s.c.-injected sodium perborate was very effectively degraded without administration of catalase,[22] suggesting that endogenous catalase can decrease the level of systemic oxidants. In mice without lung

colonies of colon 26 tumor cells, high catalase activity was detected in the liver (66,100 units/g tissue), lung (2,390 units/g tissue) and erythrocytes (6,340 units/ml blood), whose activities were much greater than or comparable to the administered dose of catalase (35,000 units/kg, *i.e.*, about 900 units/mouse). In mice with pulmonary metastasis, the catalase activity of the lung tended to decrease when expressed as activity per unit weight, from 2,390 to 1,430 units/g tissue, suggesting that tumor tissues have less catalase activity than lung tissue. Although there is high catalase activity in the liver, experimental hepatic metastasis occurs in various models and can be at least inhibited by administration of catalase derivatives (unpublished data). Therefore, the local level of H_2O_2 at sites where tumor cells metastasize, not its systemic or tissue level, appears to be critical for the stimulation of metastasis. These results suggest that a prolonged concentration of catalase in plasma is effective for inhibiting pulmonary tumor metastasis.

Irreversibly inactivated catalase or BSA showed little effect on the pulmonary metastasis of colon 26 tumor cells in either the *in vitro* incubation with tumor cells or the *in vivo* administration into mice with pulmonary metastasis. Therefore, the antimetastatic activity of catalase derivatives would be related to the enzymatic activity of catalase to degrade H_2O_2 into oxygen and water.

In conclusion, approaches to prolong the plasma half-life of catalase, *i.e.*, conjugation of PEG and injection into s.c. tissue, were revealed to augment its antimetastatic activity in experimental pulmonary metastasis. A direct effect of catalase on tumor cells was also indicated, probably due to reduced MMP activity of colon 26 tumor cells by detoxification of H_2O_2. These findings indicate that the control of catalase biodistribution is important to prevent pulmonary metastasis.

ACKNOWLEDGEMENTS

This work was supported in part by a Grant-in-Aid for Scientific Research from the Ministry of Education, Science, Sports, and Culture of Japan.

REFERENCES

1. Engers R, Gabbert HE. Mechanisms of tumor metastasis: cell biological aspects and clinical implications. J Cancer Res Clin Oncol 2000; 126:682–92.
2. Onoda JM, Piechocki MP, Honn KV. Radiation-induced increase in expression of the αIIβ3 integrin in melanoma cells: effects on metastatic potential. Radiat Res 1992;130:281–8.
3. Sellak H, Franzini E, Hakim J, Pasquier C. Reactive oxygen species rapidly increase endothelial ICAM-1 ability to bind neutrophils without detectable upregulation. Blood 1994;83:2669–77.
4. Belkhiri A, Richards C, Whaley M, McQueen SA, Orr FW. Increased expression of activated matrix metalloproteinase-2 by human endothelial cells after sublethal H_2O_2 exposure. Lab Invest 1997;77:533–9.
5. Rajagopalan S, Meng XP, Ramasamy S, Harrison DG, Galis ZS. Reactive oxygen species produced by macrophage-derived foam cells regulate the activity of vascular matrix metalloproteinases in vitro. Implications for atherosclerotic plaque stability. J Clin Invest 1996; 98:2572–9.
6. Shaughnessy SG, Whaley M, Lafrenie RM, Orr FW. Walker 256 tumor cell degradation of extracellular matrices involves a latent gelatinase activated by reactive oxygen species. Arch Biochem Biophys 1993;304:314–21.
7. Murrell GA, Francis MJ, Bromley L. Modulation of fibroblast proliferation by oxygen free radicals. Biochem J 1990;265:659–65.
8. Yang M, Nazhat NB, Jiang X, Kelsey SM, Blake DR, Newland AC, Morris CJ. Adriamycin stimulates proliferation of human lymphoblastic leukaemic cells via a mechanism of hydrogen peroxide (H_2O_2) production. Br J Haematol 1996;95:339–44.
9. Monte M, Davel LE, Sacerdote de Lustig E. Hydrogen peroxide is involved in lymphocyte activation mechanisms to induce angiogenesis. Eur J Cancer 1997;33:676–82.
10. Nonaka Y, Iwagaki H, Kimura T, Fuchimoto S, Orita K. Effect of reactive oxygen intermediates on the in vitro invasive capacity of tumor cells and liver metastasis in mice. Int J Cancer 1993;54:983–6.
11. Yoshizaki N, Mogi Y, Muramatsu H, Koike K, Kogawa K, Niitsu Y. Suppressive effect of recombinant human Cu, Zn-superoxide dismutase on lung metastasis of murine tumor cells. Int J Cancer 1994; 57:287–92.
12. Fujita T, Nishikawa M, Tamaki C, Takakura Y, Hashida M, Sezaki H. Targeted delivery of human recombinant superoxide dismutase by chemical modification with mono- and polysaccharide derivatives. J Pharmacol Exp Ther 1992;263:971–8.
13. Yabe Y, Koyama Y, Nishikawa M, Takakura Y, Hashida M. Hepatocyte-specific distribution of catalase and its inhibitory effect on hepatic ischemia/reperfusion injury in mice. Free Radic Res 1999;30: 265–74.
14. Yabe Y, Nishikawa M, Tamada A, Takakura Y, Hashida M. Targeted delivery and improved therapeutic potential of catalase by chemical modification: combination with superoxide dismutase derivatives. J Pharmacol Exp Ther 1999;289:1176–84.
15. Thakur ML, Coleman RE, Welch MJ. Indium-111-labeled leukocytes for the localization of abscesses: preparation, analysis, tissue distribution, and comparison with gallium-67 citrate in dogs. J Lab Clin Med 1997;89:217–28.
16. Liotta LA, Kleinerman J, Saidel GM. Quantitative relationships of intravascular tumor cells, tumor vessels, and pulmonary metastases following tumor implantation. Cancer Res 1974;34:997–1004.
17. Mizuno N, Kato Y, Izumi Y, Irimura T, Sugiyama Y. Importance of hepatic first-pass removal in metastasis of colon carcinoma cells. J Hepatol 1998;28:865–77.
18. Curran S, Murray GI. Matrix metalloproteinases: molecular aspects of their roles in tumour invasion and metastasis. Eur J Cancer 2000;36: 1621–30.
19. Yang M, Jiang XR, Blake DR, Zhang Z, Macey MG, Newland AC, Morris CJ. Involvement of anti-oxidant enzymes in multiple drug resistance in a human T-lymphoblastic leukemia cell line which over-express P-glycoprotein. Int J Oncol 1993;3:99–104.
20. Belkhiri A, Richards C, Whaley M, McQueen SA, Orr FW. Increased expression of activated matrix metalloproteinase-2 by human endothelial cells after sublethal H_2O_2 exposure. Lab Invest 1997;77:533–9.
21. Szatrowski TP, Nathan CF. Production of large amounts of hydrogen peroxide by human tumor cells. Cancer Res 1991;51:794–8.
22. Chang TMS, Poznansky MJ. Semipermeable microcapsules containing catalase for enzyme replacement in acatalasaemic mice. Nature 1968;218:243–5.

Am J Physiol Gastrointest Liver Physiol 282: G711–G719, 2002.
First published December 19, 2001; 10.1152/ajpgi.00358.2001.

Electrical charge on protein regulates its absorption from the rat small intestine

MAKIYA NISHIKAWA,[1] SUSUMU HASEGAWA,[1] FUMIYOSHI YAMASHITA,[1]
YOSHINOBU TAKAKURA,[2] AND MITSURU HASHIDA[1]
Departments of [1]Drug Delivery Research and [2]Biopharmaceutics, Graduate School of Pharmaceutical Sciences, Kyoto University, Sakyo-ku, Kyoto 606-8501, Japan

Received 10 August 2001; accepted in final form 12 December 2001

Nishikawa, Makiya, Susumu Hasegawa, Fumiyoshi Yamashita, Yoshinobu Takakura, and Mitsuru Hashida. Electrical charge on protein regulates its absorption from the rat small intestine. *Am J Physiol Gastrointest Liver Physiol* 282: G711–G719, 2002. First published December 19, 2001; 10.1152/ajpgi.00358.2001.—The effect of the electrical charge on the intestinal absorption of a protein was studied in normal adult rats. Chicken egg lysozyme (Lyz), a basic protein with a molecular weight of 14,300, was selected and several techniques for chemical modification were applied. Then the intestinal absorption of Lyz derivatives was evaluated by measuring the radioactivity in plasma and tissues, after the administration of an ^{111}In-labeled derivative to an in situ closed loop of the jejunum. After the administration of ^{111}In-Lyz, the level of radioactivity in plasma was comparable with the lytic activity of Lyz, supporting the fact that the radioactivity represents intact Lyz. ^{111}In-cationized Lyz showed a 2–3 times higher level of radioactivity in plasma, whereas the radioactivity of ^{111}In-anionized Lyz was much lower. The absorption rate of ^{111}In-Lyz derivatives calculated by a deconvolution method was correlated for the strength of their positive net charge. A similar relationship was observed using superoxide dismutase. These findings indicate that the intestinal absorption of a protein is, at least partially, determined by its electrical charge.

intestinal absorption; chicken egg lysozyme; pharmacokinetics; chemical modification; superoxide dismutase

INTESTINAL PERMEABILITY IS known to be altered in disease states such as Crohn's disease, celiac disease, viral infection, and multiple organ failure (38, 42, 47). Under these abnormal conditions, not only low-molecular weight compounds but also macromolecules, such as proteins, can pass transcellularly or paracellularly through the intestinal epithelium and be absorbed into the circulation. Altered properties of the intestinal epithelial cells would explain the difference in permeability. Such changes lead to the increased nonspecific adsorption of proteins to the cell (42). Increased permeability of macromolecules is related to the symptoms observed in these diseases.

However, in healthy adults, it is well known that the intestinal permeability of a solute through the intercellular junction (paracellular pathway) is highly dependent on its molecular size (6, 15). Molecules that hardly interact with intestinal tissue might exhibit a simple correlation between their molecular size and rate and extent of absorption. Therefore, the intestinal epithelium of healthy adults is generally considered to be virtually impermeable to macromolecules. In addition to this mechanical barrier presented by the tissue, the enzymatic barrier, i.e., a rapid and extensive degradation of proteins by digestive enzymes, highly restricts the entry of intact, undigested proteins into the body (42). However, some studies support the idea that there is a small, but significant, degree of transport of biologically and/or antigenically active peptides and proteins through the epithelial cells of the intestines (2, 5, 17, 25, 41). The mechanism of this transport through the intestines has received little attention to date.

Intestinal epithelial cells possess a negatively charged cell surface as do other types of cells. The charged surface provides sites of interaction for positively charged compounds. Because of this charge-based interaction, cationic macromolecules have been used to increase the delivery of drugs and genes to target cells (3, 4). Positive charges on the molecular surface can be electrostatically attracted and adsorbed to the negatively charged cell surface glycoproteins, followed by increased cellular uptake of the positively charged molecules. These findings suggest that electrostatic interaction of protein with the intestinal epithelial cells may be a factor determining its intestinal absorption. However, there are few investigations of the intestinal absorption of proteins that have considered the electrical charge. Proteins formulated in oral dosage forms include positively charged ones, such as lysozyme, bromelain, and pancreatopeptidase E. The cationic nature of these protein drugs could facilitate their interaction with intestinal tissue, resulting in detectable absorption from the intestine (5). The effect of the electrical charge of proteins on their intestinal absorption needs to be quantitatively investigated.

To this end, we chose chicken egg lysozyme (Lyz) as a model positively charged protein (isoelectric point of

Address for reprint requests and other correspondence: M. Hashida, Dept. of Drug Delivery Research, Graduate School of Pharmaceutical Sciences, Kyoto University, Sakyo-ku, Kyoto 606-8501, Japan (E-mail: hashidam@pharm.kyoto-u.ac.jp).

The costs of publication of this article were defrayed in part by the payment of page charges. The article must therefore be hereby marked "*advertisement*" in accordance with 18 U.S.C. Section 1734 solely to indicate this fact.

11) with a molecular weight of 14,300, because it can be absorbed from the intestines in small quantities (53, 54). Its electrical charge is altered by chemical modification, i.e., coupling with hexamethylenediamine or succinic anhydride to endow Lyz with an additional positive charge or negative charge, respectively. In addition, galactose or glucose can be covalently attached to Lyz to give glycosylated derivatives, because the intestinal epithelial cells possess glucose transporters, and some reports (23, 30) suggested their involvement in the enhanced absorption of glycosylated molecules. Pharmacokinetic profiles of these derivatives radiolabeled with ^{111}In were studied in rats after intrajejunal administration or intravenous injection. The absorption rate was estimated by a deconvolution method using the profiles of the concentrations in plasma after intravenous and intrajejunal administration, and the relationship between the electrical charge of the protein derivatives and their absorption rate from the intestine was examined. In addition, to examine whether the relationship obtained can be applied to other proteins, we also report the altered intestinal absorption properties of recombinant human superoxide dismutase (SOD) that is different from Lyz in its physicochemical properties such as the electrical charge (negative, isoelectric point of ~5) and molecular weight (32,000) after cationization.

MATERIALS AND METHODS

Animals. Male Wistar rats (180–210 g) were purchased from the Shizuoka Agricultural Cooperative Association for Laboratory Animals (Shizuoka, Japan). Rats were fasted for 20 h before experimentation. All procedures were examined by the Ethics Committee on Animal Experimentation at Kyoto University.

Chemicals. Chicken egg Lyz and FITC were purchased from Sigma (St. Louis, MO). Recombinant human SOD (^{111}Ser) was supplied by Asahi Chemical (Shizuoka, Japan). Diethylenetriaminepentaacetic acid (DTPA) anhydride was purchased from Dojindo Laboratory (Kumamoto, Japan). $^{111}InCl_3$ was supplied by Nihon Medi-Physics (Takarazuka, Japan). *Micrococcus lysodeikticus* was purchased from Nacalai Tesque (Kyoto, Japan). All other chemicals were obtained commercially as reagent-grade products.

Synthesis of Lyz and SOD derivatives. Anionized Lyz (An-Lyz) was synthesized by succinylation (51), i.e., by reacting succinic anhydride with the amino group of Lyz. Coupling 1,6-hexamethylenediamine to Lyz was performed with 1-ethyl 3-(3-dimethylaminopropyl)carbodiimide to obtain highly positively charged Lyz [cationized Lyz (Cat-Lyz)] (49). Glucosylated (Glc-Lyz) and galactosylated Lyz (Gal-Lyz) were synthesized by reacting Lyz with 2-imino-2-methoxyethyl 1-thioglucoside or thiogalactoside, respectively, according to the method of Lee et al. (24). Highly negatively charged SOD [anionized SOD (An-SOD)] and cationized SOD (Cat-SOD) were synthesized by the same method as An-Lyz and Cat-Lyz, respectively.

The number of amino groups in each derivative was determined by trinitrobenzene sulfonic acid using glycine as a standard (11). The number of sugar residues was determined by the anthron-sulfuric acid method. The molecular weight of Lyz derivatives was estimated by SDS-PAGE using a standard curve obtained with marker proteins (low-range marker; Wako, Osaka, Japan), and that of SOD derivatives was estimated by HPLC gel-filtration chromatography using Shim-pack Diol-300 column (Shimadzu, Kyoto, Japan). Electrophoretic mobility of Lyz and SOD derivatives was measured with a laser electrophoresis-zeta potential analyzer (LEZA-500T; Otsuka Electronics). The lytic activity of Lyz derivatives was measured using *M. lysodeikticus* according to the method of Selsted and Martinez (45).

Labeling. Lyz and SOD derivatives were radiolabeled with ^{111}In using the bifunctional chelating agent, DTPA anhydride, according to the method of Hnatowich et al. (16). In brief, protein (2 mg) was dissolved in 1 ml 4-(2-hydroxyethyl)-1-piperazinethane sulfonic acid buffer (0.1 M, pH 7.0) and a twofold molar excess of DTPA anhydride in 10 μl dimethyl sulfoxide was added. After stirring for 30 min at room temperature, the mixture was purified by gel-filtration chromatography using a Sephadex G-25 column (1 × 40 cm) and eluted with acetate buffer (0.1 M, pH 6.0) to separate unreacted DTPA. Fractions containing DTPA-coupled protein were selected using spectrophotometry and concentrated by ultrafiltration. Thirty microliters $^{111}InCl_3$ solution was added to 30 μl sodium acetate buffer (1 M, pH 6.0), and 60 μl DTPA-protein derivative was then added to the mixture. After 30 min at room temperature, the mixture was purified by gel filtration chromatography using a PD-10 column (Amersham Pharmacia Biotech, Uppsala, Sweden) and eluted with acetate buffer (0.1 M, pH 6.0). The appropriate fractions were selected based on their radioactivity and concentrated by ultrafiltration. The specific activity of the obtained samples was ~40 MBq/mg protein.

Separately, FITC was coupled to Lyz derivatives by the method of Monsigny et al. (31) for confocal fluorescence microscopic studies.

Biodistribution after intravenous injection. Rats were anaesthetized by intraperitoneal injection of pentobarbital sodium (50 mg/kg). The urinary bladder and bile duct were cannulated for the collection of bile and urine samples. ^{111}In-Lyz derivative was injected into the femoral vein at a dose of 0.1 mg/kg. At predetermined time points, blood, urine, and bile were collected for the entire experimental period (3 h). At the end, rats were killed, and the liver, kidney, and spleen were sampled. Blood samples were centrifuged at 2,000 *g* for 2 min, and 100 μl plasma was assayed for radioactivity.

Intestinal absorption from an in situ closed loop. Intestinal absorption of the test compound was examined in the in situ closed loop of the jejunum. A midline abdominal incision was made, and the lumen of the jejunum was washed with saline three times. A jejunal loop, 5 cm in length, was prepared by closing both ends with sutures. Each protein derivative was dissolved in 700 μl phosphate buffer (0.15 M, pH 6.5) and then administered into the jejunal loop at a dose of 1 or 10 mg/kg body wt. Blood, urine, and bile samples were collected for 3 h.

Degradation of ^{111}In-Lyz derivatives in the loop was examined in different rats. At 30 min, 1 or 3 h after intrajejunal administration, the contents of the loop were subjected to gel-filtration chromatography on a Sephadex G-50 column (1 × 40 cm) and eluted with MES buffer (0.05 M, pH 6.0).

Determination of ^{111}In radioactivity and lytic activity of Lyz derivatives. ^{111}In radioactivity in each sample was measured in a well-type NaI scintillation counter (ARC-500, Aloka, Tokyo). Lytic activity of Lyz and Cat-Lyz in plasma was measured using *M. lysodeikticus* as described above.

Confocal microscopic images. FITC-Lyz derivatives were introduced into the loop in the same manner as in the in situ absorption experiment. At 1 h after administration, rats were killed and the loop was excised, washed with PBS, and frozen. Cryosections 10-μm thick were made using a cryostat

(CM3000-Kryostat; Leica, Heidelberg, Germany) and fixed with 4% formaldehyde; the nucleus was stained with propidium iodide. Slices were scanned with a confocal laser microscope (ACAS 570 interactive laser cytometer; Meridian Instruments).

Estimation of amount absorbed by deconvolution method. Plasma concentration of ^{111}In-protein after intrajejunal administration [$C_{po}(t)$] is expressed as follows (39)

$$C_{po}(t) = \int_0^t f(\theta)C_{iv}(t-\theta)d\theta \quad (1)$$

where $f(t)$ is an absorption rate at *time t* and $C_{iv}(t)$ is the plasma concentration at *time t* after intravenous injection of an unit dose (an impulse input). When the amount of $f(\theta)\Delta\theta$ is rapidly injected to the systemic circulation at *time* θ, plasma concentration associated with the pulse is $f(\theta)\Delta\theta C_{iv}(t-\theta)$ at *time t*. *Equation 1* is derived, considering that an absorption rate-time profile is composed of an infinite number of the input pulses. Absorption profiles of ^{111}In-protein were estimated by deconvoluting $C_{po}(t)$ with $C_{iv}(t)$ in *Eq. 1* (20). In applying the computation algorithm (20), the plasma concentration-time profile of radioactivity after intravenous injection of ^{111}In-protein was approximated with a biexponential equation.

Statistical analysis. Differences were statistically evaluated by one-way ANOVA followed by the Student-Newman-Keuls multiple comparison test. The level of significance was set at $^{*}P < 0.05$ and $^{**}P < 0.01$.

RESULTS

Physicochemical characteristics of Lyz derivatives. The physicochemical characteristics of Lyz derivatives are summarized in Table 1. All synthesized Lyz derivatives had a similar molecular size to unmodified Lyz. The number of free amino groups in Lyz fell from 7.8 to 1.4 for An-Lyz and to 2.5 for Glc- and Gal-Lyz, whereas the number increased to 10.5 for Cat-Lyz. Lyz had an electrophoretic mobility of 0.14×10^{-4} cm^2·V^{-1}·s^{-1} at pH 6.5, after determination by a zeta potential analyzer. The mobility increased by cationization to 0.56×10^{-4} cm^2·V^{-1}·s^{-1}. On the other hand, An-Lyz was electrophoresed to the positive pole, indicating its negative surface charge (-0.52×10^{-4} cm^2·V^{-1}·s^{-1}). These determinations confirmed that Cat-Lyz is a highly cationic derivative of Lyz, whereas An-Lyz is an anionic derivative. Glycosylation slightly reduced the positive charge of Lyz. Lytic activity was almost unchanged for Cat-, Glc-, and Gal-Lyz. However, succinylation of Lyz (An-Lyz) resulted in a complete loss of enzymatic activity, suggesting the cationic charge of Lyz is critical for its lytic activity.

Disposition of ^{111}In-Lyz derivatives after intravenous injection. The tissue disposition of ^{111}In-Lyz derivatives was examined after intravenous bolus injection into rats. Figure 1A shows the plasma concentration-time profile of radioactivity after intravenous injection at a dose of 0.1 mg/kg into rats. ^{111}In-Lyz rapidly disappeared from plasma. Chemical modification of Lyz slightly altered the elimination rate from plasma and had a marked effect on the tissue disposition of ^{111}In-Lyz (Fig. 1, *B–F*). ^{111}In-Lyz was recovered largely in the kidneys (53% of dose) and urine (20%) but not in the liver (1.9%), reflecting its high susceptibility to glomerular filtration and reabsorption (18, 26). ^{111}In-An-Lyz was largely excreted into urine instead of accumulating in the kidney, whereas ^{111}In-Cat-Lyz was recovered in both the liver (31%) and kidney (54%). ^{111}In-Gal-Lyz and ^{111}In-Glc-Lyz also showed high hepatic recovery in addition to recovery in the kidney and urine, suggesting their recognition by the asialoglycoprotein receptors on hepatocyte (34).

Tissue disposition of ^{111}In-Lyz after intrajejunal administration. ^{111}In-Lyz was administered into the jejunal loop, and the contents of the loop were applied to a column to check the molecular size of ^{111}In-Lyz. ^{111}In-Lyz recovered at 0.5 and 1 h after its administration into the jejunal loop showed a similar chromatographic profile to that of intact ^{111}In-Lyz. At the end of the 3-h experiment, ~3% of the radioactivity was eluted in fractions different from those of ^{111}In-Lyz (data not shown).

Figure 2*A* shows the plasma concentration-time profile of radioactivity after intrajejunal administration of ^{111}In-Lyz derivatives at a dose of 1 mg/kg. Radioactivity was detected in plasma after intrajejunal administration of ^{111}In-Lyz, indicating that ^{111}In-Lyz can be

Table 1. *Physicochemical properties of Lyz and SOD derivatives*

Compound	Molecular Weight	Number of amino (Sugar) Groups	Enzymatic Activity, % with respect to original	Electrophoretic Mobility at pH 6.5, 10^{-4} cm^2·V^{-1}·s^{-1}
Lyz	14,300	7.8	100	0.137 ± 0.058
An-Lyz	14,600	1.4	ND	−0.517 ± 0.169
Cat-Lyz	15,000	10.5	100	0.556 ± 0.060
Glc-Lyz	15,000	2.5(4.3)	105	0.052 ± 0.021
Gal-Lyz	15,000	2.5(4.4)	106	0.048 ± 0.009
SOD	32,000	24	100	−0.461 ± 0.025
Cat-SOD	34,000	35	47	0.106 ± 0.056

The molecular weight of lysozyme (Lyz) and superoxide dimutase (SOD) derivatives was estimated by SDS-PAGE or by HPLC gel chromatography, respectively. The number of amino groups was measured with trinitrobenzene sulfonic acid using glycine as a standard (11). The number of sugar residues was determined by the anthron-sulfuric acid method. Enzymatic activity of Lyz was measured using *Micrococcus lysodeikticus* (45), and that of SOD was determined by a nitroblue tetrazolium reduction method. Electrophoretic mobility was measured using a laser electrophoresis-zeta potential analyzer (model LEZA-500T, Otsuka Electronics). An, anionized; Cat, cationized; Glc, glucosylated; Gal, galactosylated; ND, not detected.

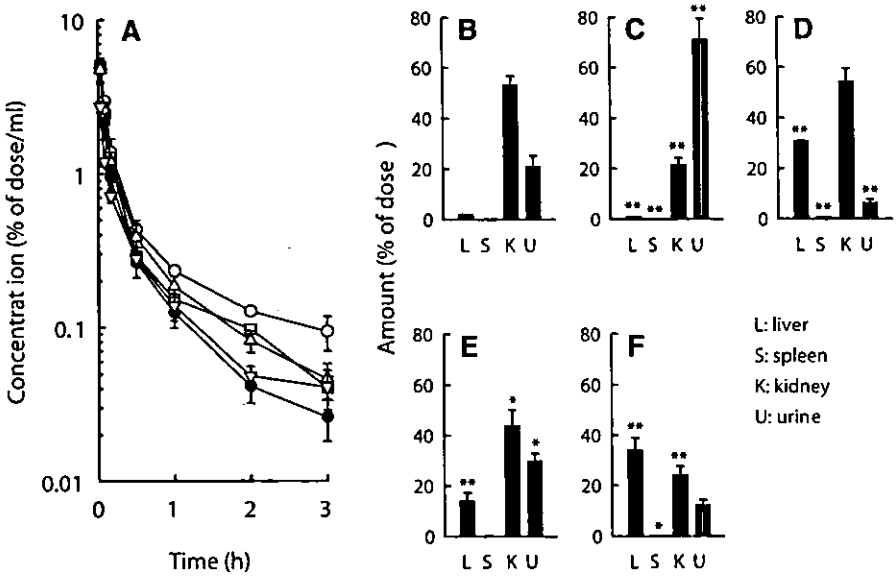

Fig. 1. Plasma concentration-time course (*A*) and tissue disposition at 3 h (*B-F*) of radioactivity after intravenous injection of ^{111}In-Lyz derivatives into rats at a dose of 0.1 mg/kg. ○, *B*, ^{111}In-Lyz; ●, *C*, ^{111}In-An-Lyz; □, *D*, ^{111}In-Cat-Lyz; △, *E*, ^{111}In-Glc-Lyz; ▽, *F*, ^{111}In-Gal-Lyz. Results are expressed as means ± SD of 3 rats. $*P < 0.05$ and $**P < 0.01$, statistically significant difference from ^{111}In-Lyz. The concentration of ^{111}In-Lyz derivatives in plasma was also significantly different from ^{111}In-Lyz although not marked in the figure: ^{111}In-An-Lyz ($P < 0.05$ for 5 min, 3 h; $P < 0.01$ for 30 min, 1 and 2 h); ^{111}In-Cat-Lyz ($P < 0.05$ for 30 min, 3 h; $P < 0.01$ for 1 and 2 h); ^{111}In-Glc-Lyz ($P < 0.05$ for 1 and 3 h; $P < 0.01$ for 2 h); and ^{111}In-Gal-Lyz ($P < 0.05$ for 10, 30 min, and 3 h; $P < 0.01$ for 2 and 5 min, 1 and 2 h). Lyz, lysozyme; An, anionized; Cat, cationized; Glc, glucosylated; Gal, galactosylated.

absorbed from the intestine. Compared with ^{111}In-Lyz, ^{111}In-Cat-Lyz showed a two- to threefold higher level of radioactivity in plasma ($P < 0.05$ at 2 h, $P < 0.01$ at 1 and 3 h). On the other hand, ^{111}In-An-Lyz showed much less radioactivity, although the difference was not significant. The plasma level of radioactivity after the administration of the ^{111}In-glycosylated Lyz derivatives was a little lower than that of ^{111}In-Lyz. The tissue disposition profiles of radioactivity after intrajejunal administration of the ^{111}In-Lyz derivatives were similar to those obtained after administration by the intravenous route (Fig. 2, *B–F*). These tissue disposition data after intrajejunal administration suggest that Lyz derivatives retain their structural characteristics even after passage through the intestinal epithelial cells into the blood circulation.

When the tissue disposition was normalized with respect to the dose (%dose or %dose/ml), no significant differences were observed in the tissue disposition of radioactivity after intrajejunal administration of ^{111}In-Lyz or ^{111}In-Cat-Lyz at a dose of 1 and 10 mg/kg (Fig. 3). For both derivatives, the disposition profiles at the 10 mg/kg dose could be superimposed on those obtained at the 1 mg/kg dose, indicating that the intestinal absorption of these Lyz derivatives is proportional to the dose over the range examined.

To see whether the absorbed fraction of ^{111}In-Lyz remains intact, the lytic activity of Lyz in plasma after intrajejunal administration of (nonradiolabeled) Lyz was examined at a dose of 10 mg/kg. The concentration of lytic activity in plasma was comparable with, and not significantly different from, the concentration of ^{111}In radioactivity after ^{111}In-Lyz administration, after their normalization to the administration dose (Fig. 4). These results suggest that the radioactivity in plasma after administration of ^{111}In-Lyz is due to intact Lyz.

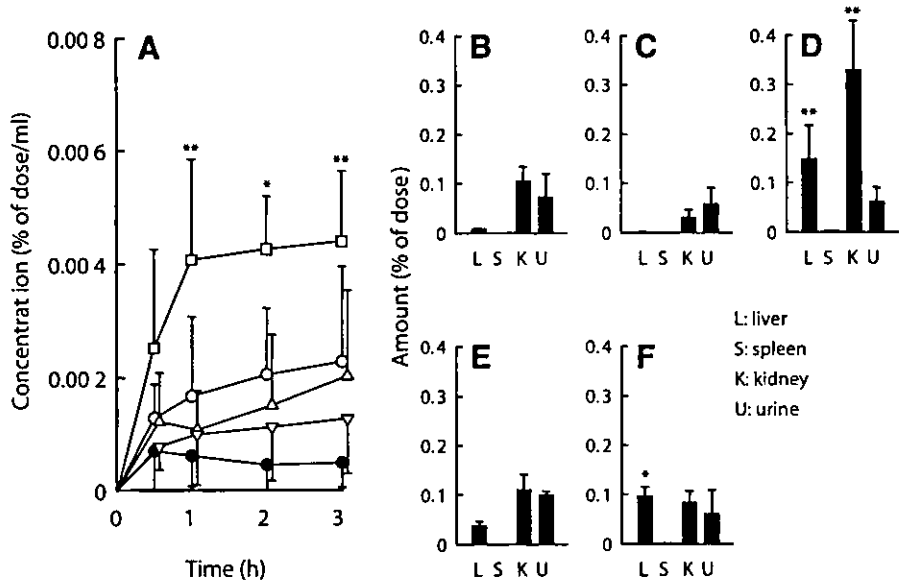

Fig. 2. Plasma concentration-time course (*A*) and tissue disposition at 3 h (*B-F*) of radioactivity after intrajejunal administration of ^{111}In-Lyz derivatives into rats at a dose of 1 mg/kg. ○, *B*, ^{111}In-Lyz; ●, *C*, ^{111}In-An-Lyz; □, *D*, ^{111}In-Cat-Lyz; △, *E*, ^{111}In-Glc-Lyz; ▽, *F*, ^{111}In-Gal-Lyz. Results are expressed as means ± SD of 3 (^{111}In-An-Lyz), 4 (^{111}In-Lyz, ^{111}In-Cat-Lyz, ^{111}In-Gal-Lyz), or 6 (^{111}In-Glc-Lyz) rats. $*P < 0.05$ and $**P < 0.01$, statistically significant difference from ^{111}In-Lyz.

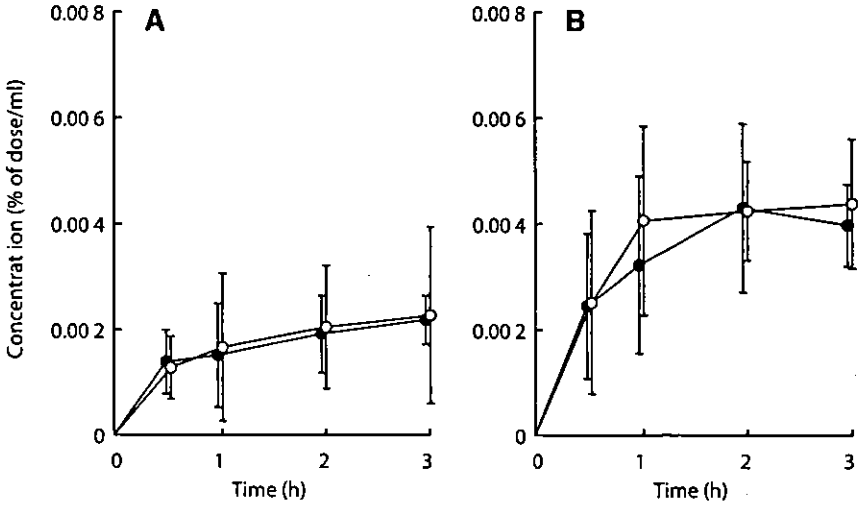

Fig. 3. Dose dependence of plasma concentration-time course of radioactivity after intrajejunal administration of ^{111}In-Lyz (*A*) and ^{111}In-Cat-Lyz (*B*) into rats at a dose of 1 or 10 mg/kg. ○, 1 mg/kg; ●, 10 mg/kg. Results are expressed as means ± SD of 3 (10 mg/kg) or 4 (1 mg/kg) rats.

Confocal microscopic images of rat jejunum after administration of FITC-Lyz derivatives. Figure 5 shows the confocal microscopic images of rat jejunum cryosections after intrajejunal administration of FITC-Cat-Lyz. Green fluorescence derived from FITC-Cat-Lyz was mainly observed around the luminal surface of the tissue. In addition, fluorescence could be detected near the nucleus of the epithelial cells. Fluorescent intensity associated with the intestinal tissue depended on the electrical charge of the Lyz derivative, and FITC-An-Lyz had a much weaker signal (data not shown).

Intestinal absorption rate of ^{111}In-Lyz derivatives calculated by deconvolution method. Intestinal absorption-time courses of ^{111}In-Lyz derivatives were calculated by a deconvolution method using the plasma concentration-time profiles after intravenous and intrajejunal administration (Fig. 6). ^{111}In-Lyz derivatives were linearly absorbed from the jejunum with time. The amount of ^{111}In-Cat-Lyz absorbed was significantly greater than that of ^{111}In-Lyz ($P < 0.05$ at 1, 2, and 3 h), which resulted in a greater absorption rate for ^{111}In-Cat-Lyz (0.46% dose/h) (Table 2). On the other hand, the absorption of ^{111}In-An-Lyz was much slower than that of the cationic derivatives, although the difference was not significant. The rates of ^{111}In-Gal-Lyz and ^{111}In-Glc-Lyz were calculated and found to be comparable with that of ^{111}In-Lyz, indicating that glycosylation has no effect on the intestinal absorption of Lyz.

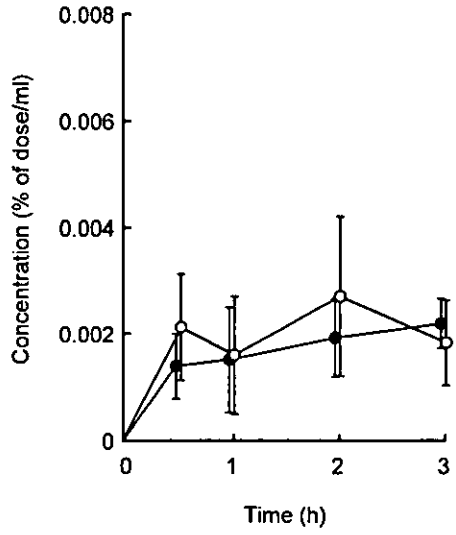

Fig. 4. Comparison of radioactivity and lytic activity of Lyz after intrajejunal administration of ^{111}In-Lyz and Lyz, respectively, into rats at a dose of 10 mg/kg. ○, lytic activity; ●, ^{111}In radioactivity. Results are expressed as means ± SD of 4 (^{111}In radioactivity) or 3 (lytic activity) rats.

Intestinal absorption of ^{111}In-SOD derivatives. Table 1 shows the physicochemical characteristics of SOD and Cat-SOD. After intrajejunal administration of ^{111}In-SOD and ^{111}In-Cat-SOD, low but significant radioactivity was detected in plasma (data not shown). However, in the case of ^{111}In-An-SOD, there was no detectable radioactivity in plasma throughout the experiment that lasted 3 h. Figure 7 shows the intestinal absorption-time courses of ^{111}In-SOD and ^{111}In-Cat-SOD. Although ^{111}In-Cat-SOD tended to be more absorbed from the intestine than ^{111}In-SOD, the amount absorbed was not significantly different except for the first time point ($P < 0.05$). The absorption rate calculated for ^{111}In-Cat-SOD was twofold greater than that for ^{111}In-SOD (Table 2), but these values were less than those exhibited by the ^{111}In-Lyz derivatives, probably reflecting the differences in the properties of SOD and Lyz, e.g., the molecular size (32,000 SOD; 14,300 Lyz).

DISCUSSION

Cationization is a universal approach applied to increase the interaction of compounds with negatively charged biological components. Since Felgner (8) reported efficient gene expression using cationic lipids for the transfection of cells with plasmid DNA, cationic molecule-based delivery systems for plasmid DNA have been extensively investigated in an attempt to achieve nonviral gene transfer to target cells (33). In addition, enzymes such as SOD (27, 28, 40, 48), glucose

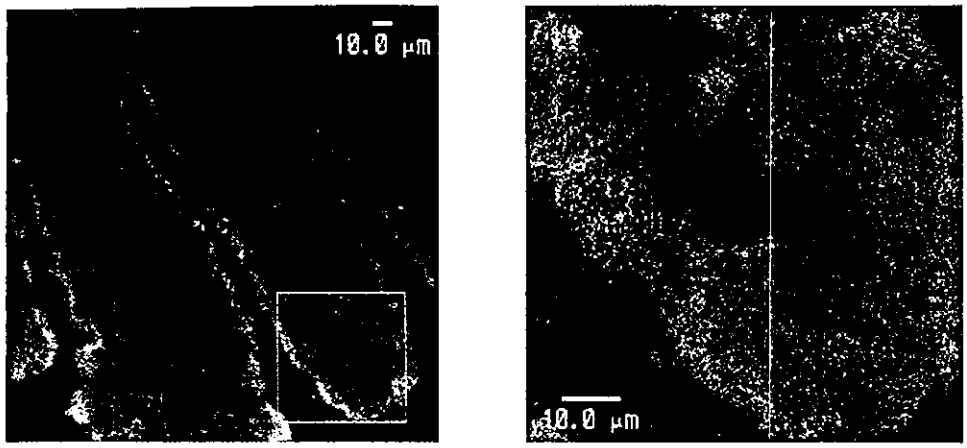

Fig. 5. Confocal microscopic images of cryosections of the rat jejunum after intrajejunal administration of FITC-Cat-Lyz to rats. Nuclei of cells were stained with propidium iodide. *Left*, ×169 maginification; *right*, ×564 magnification of rectangular area indicated by the white line, *left*.

oxidase (21), and catalase (21, 43), as well as serum albumins (32), immunoglobulins (52), and ferritin (7), all of which are negatively charged at physiological pH, have been directly modified with diamines to obtain cationized derivatives. Cationized proteins exhibit increased cellular uptake by brain microvascular endothelial cells, hepatocytes, kidney epithelial cells, and enterocytes. On interaction with the negatively charged surface of cells, cationized proteins are believed to be endocytosed or transcytosed through an adsorptive endocytosis/transcytosis process. However, to our knowledge, there have been few studies to examine the effect of the electrical charge of a protein on its intestinal absorption. Intestinal epithelial cells possess a negatively charged surface like other cells. Therefore, in the present study, the effect of the physicochemical properties, especially the electrical charge, of the protein on its intestinal absorption was explored using an in situ closed loop of rat jejunum. In this system, the pH of the solution in the loop could hardly change from the initial value of pH 6.5 during experiment, and the local luminal pH might not be so different from the pH value of the bulk solution (22).

A reliable detection method is required to evaluate the intestinal absorption of proteins. We carried out ^{111}In labeling using DTPA anhydride to monitor the disposition of proteins because of the better stability of these radiolabeled proteins compared with their iodinated counterparts (13, 36). A possible radioactive metabolite, ^{111}In-DTPA-lysine (9), has only a limited capacity to cross biological membranes and to escape from cells where the labeled protein is degraded after endocytosis. When Lyz was radioiodinated and administered to the rat jejunal loop, the concentration of trichloroacetic acid-precipitable ^{125}I radioactivity in plasma was higher than that of ^{111}In radioactivity after the administration of ^{111}In-Lyz (data not shown). When radioiodinated Lyz was used for experiments, the concentration of radioactivity in plasma was much greater than one obtained with ^{111}In counterpart ($P < 0.01$). Finding no significant differences between the lytic activity of Lyz and ^{111}In radioactivity strongly supports the idea that the transport of intact Lyz derivatives through the intestinal epithelium can be assayed by monitoring ^{111}In radioactivity. These considerations suggest that radioiodination might overes-

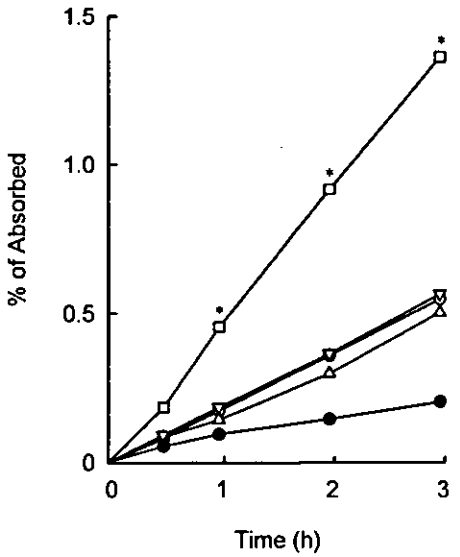

Fig. 6. Intestinal absorption time courses of ^{111}In-Lyz derivatives calculated by a deconvolution method. ○, ^{111}In-Lyz; ●, ^{111}In-An-Lyz; □, ^{111}In-Cat-Lyz; △, ^{111}In-Glc-Lyz; ▽, ^{111}In-Gal-Lyz. *$P < 0.05$, statistically significant difference from ^{111}In-Lyz.

Table 2. *Intestinal absorption rate of ^{111}In-Lyz and ^{111}In-SOD derivatives following intrajejunal administration to rats calculated by a deconvolution method*

Compound	Absorption rate, % of dose/h	Apparent permeability coefficient × 10^{-7} (cm/s)
Lyz	0.184 ± 0.002	0.539
An-Lyz	0.065 ± 0.006	0.191
Cat-Lyz	0.462 ± 0.009	1.35
Glc-Lyz	0.165 ± 0.008	0.484
Gal-Lyz	0.187 ± 0.002	0.548
SOD	0.025 ± 0.002	0.0733
Cat-SOD	0.056 ± 0.003	0.164

Results are expressed as the means ± SD. The apparent permeability coefficient is calculated by dividing the estimated absorption rate by the area of exposed intestine (6.63 cm^2) and the initial concentration (100% of dose/0.7 ml).

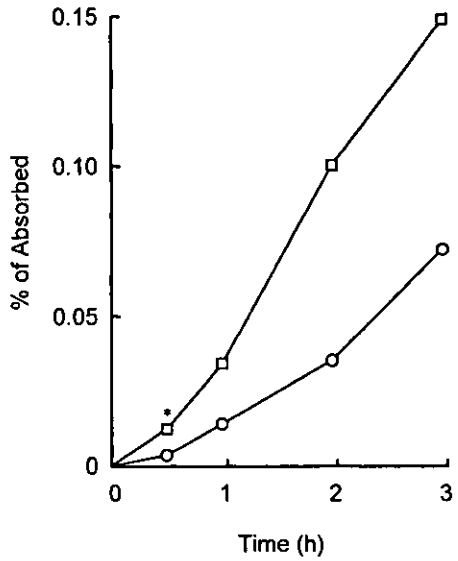

Fig. 7. Intestinal absorption time courses of ^{111}In-SOD and ^{111}In-Cat-SOD calculated by a deconvolution method. ○, ^{111}In-SOD; □, ^{111}In-Cat-SOD. *$P < 0.05$, statistically significant difference from ^{111}In-Lyz. SOD, superoxide dismutase.

timate the intestinal absorption of proteins, although the reason for the discrepancy needs to be understood.

Chemical modification greatly changed the tissue disposition characteristics of Lyz after intravenous injection. As summarized in our reviews (14, 46, 50), the tissue disposition of macromolecules is determined mainly by the overall physicochemical properties, such as the electrical charge and molecular weight, as well as by the structure involved in the specific recognition, such as monoclonal antibody, lectin, and sugar. Macromolecules having a molecular size smaller than the threshold of the glomerular filtration of the kidney are easily filtered and then reabsorbed at the proximal tubules depending on their property (26). This is the case for Lyz and SOD, and the cationic nature of Lyz increases the susceptibility to glomerular filtration and reabsorption. When ^{111}In-Lyz was injected intravenously, the radioactivity was mainly recovered in the kidney and urine (Fig. 2). ^{111}In-Cat-Lyz, which has about fourfold greater mobility to the negative pole than Lyz, showed a relatively high accumulation in the liver, like other cationic proteins, such as cationized bovine serum albumin (32). No detectable oligomers formed during the cationization were found during SDS-PAGE (data not shown). On the other hand, succinylation of Lyz greatly altered the balance of radioactivity in the kidney and urine. Because the renal uptake of macromolecules occurs mainly from the luminal side of epithelial cells (26) and not from the capillary side, such changes indicate that the reabsorption of Lyz is inhibited by succinylation. Both ^{111}In-glycosylated Lyz derivatives showed some hepatic uptake after systemic administration. Hepatocytes are known to possess asialoglycoprotein receptors on their surface that recognize compounds having galactose or *N*-acetylgalactosamine at the nonreducing end of the sugar chain (1). Synthetically galactosylated macromolecules are ligands for the receptor (34), and this is the reason for the high hepatic uptake of ^{111}In-Gal-Lyz. Although asialoglycoprotein receptors have a much lower affinity for glucose than galactose, it binds to proteins modified with 2-imino-2-methoxyethyl 1-thioglucoside as used in the present study. Therefore, asialoglycoprotein receptors are involved in the hepatic uptake of ^{111}In-Glc-Lyz (34). Although the imidination used in this study to synthesize glycosylated Lyz has been reported not to alter the electrical charge of the protein (24), their electrophoretic mobility was a little lower than that of Lyz, suggesting a reduced positive charge after glycosylation. These glycosylated derivatives were prepared because: *1*) these modified derivatives possess a positive charge intermediate between unmodified Lyz and An-Lyz and *2*) some reports have suggested the involvement of specific mechanisms for sugars associated with enterocytes as far as the transport of glycosylated macromolecules is concerned (12, 23).

The tissue disposition profile of radioactivity after intrajejunal administration of each ^{111}In-Lyz derivative was comparable with that after intravenous administration (Figs. 1 and 2), suggesting that Lyz derivatives entering the systemic circulation from the intestine possess unique physicochemical properties. Tissue uptake clearances, which can be calculated based on the area under the plasma concentration-time curve and the amount in tissue (35), were also comparable after intravenous and intrajejunal administration (data not shown). These results indicate that the radioactive molecules appearing in the plasma maintain the structures that determine their tissue disposition.

There have been reports showing that some proteins can be absorbed from the intestinal tract, although

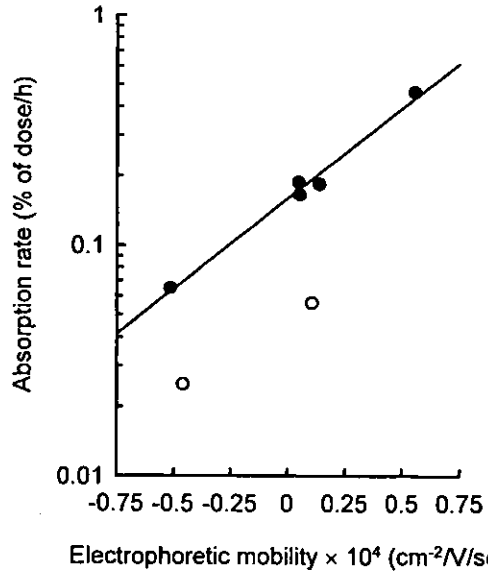

Fig. 8. Dependence of the intestinal absorption rate of ^{111}In-Lyz and ^{111}In-SOD derivatives on the electrophoretic mobility measured by a zeta sizer. ●, ^{111}In-Lyz derivatives; ○, ^{111}In-SOD derivatives. The absorption rate of a derivative calculated by the deconvolution method is plotted against its electrophoretic mobility.

skepticism about the experimental evidence of transmucosal absorption of proteins is common because of the limitations of the methodology used (44). Recently, Castell et al. (5) clearly showed that bromelain, a basic protein with a molecular mass of 24–26 kDa isolated from the stem of the pineapple plant, can be absorbed from the intestinal tract of healthy volunteers as an immunoreactive form of unchanged molecular mass. The consistency of their results indicates that the absorption of a certain protein molecule from the gastrointestinal tract is probably a common phenomenon in healthy adults. As discussed above, the cationic nature of this protein could help its intestinal absorption, although the route of its absorption, i.e., transcellular or paracellular, needs to be identified.

Cationization of Lyz did increase the intestinal absorption of Lyz, probably through the increase in the isoelectrical point of the enzyme whose positive charges result in an electrostatic attraction to the negatively charged proteoglycans of the cell surface, a process that can lead to adherence to the oppositely charged surfaces (4). Interaction of proteins with the intestinal tissues was facilitated by cationization (21, 40). Because binding to the surface can be considered as the first step in the intestinal transport of proteins, cationization might be one possible approach to increase the permeability of proteins. Increased binding of Cat-Lyz was detected in the specimens of intestinal tissues treated with FITC-labeled Lyz derivatives.

Recently, glycosylation has been applied to peptides to increase their transport across the intestinal tissues via a Na^+/glucose cotransporter (30), as well as to produce increased stability to peptidases (29). Although some reports have suggested involvement of these mechanisms in the transport of glycosylated macromolecules (12, 23), no improved absorption was observed for glycosylated Lyz derivatives. Kim et al. (19) reported that bile acid-conjugated small peptides could bind to intestinal bile acid transporters without being transported.

The amount of ^{111}In-Cat-Lyz absorbed was significantly greater than that of ^{111}In-Lyz ($P < 0.05$ at 1, 2, and 3 h), whereas that of ^{111}In-An-Lyz was smaller. The absorption rate of Lyz derivatives was proportional to their electrophoretic mobility (Fig. 8). These results clearly indicate that the electrical charge of Lyz determines its intestinal absorption from the jejunal loop. The apparent permeability coefficient of ^{111}In-Cat-Lyz (0.135×10^{-6} cm/s, Table 2), however, was still much smaller than that of small molecules such as a vasopressin derivative (43×10^{-6} cm/s, molecular weight of 1,069) and inulin (4×10^{-6} cm/s, molecular weight of 5,200) (37). The relationship between the electrical charge and intestinal absorption could also be applied to other proteins such as SOD. ^{111}In-Cat-SOD tended to be absorbed faster than ^{111}In-SOD, although the amount absorbed was not significantly different at later time points. With these protein derivatives, it is quite obvious that the molecular weight is a very important factor determining their intestinal absorption. Although ^{111}In-Cat-SOD had a greater electrophoretic mobility to the negative pole than ^{111}In-Lyz, its absorption rate was smaller than that of ^{111}In-Lyz, showing the importance of the molecular weight of the protein as far as its intestinal absorption is concerned. It is difficult to conclude that these protein derivatives are absorbed through the transcellular or paracellular route. The absorption through the both routes could be enhanced by cationization (10, 42). Further studies are needed to clarify the contribution of each route to the intestinal absorption of the derivatives.

In conclusion, it has been shown that the intestinal absorption of a protein is regulated by its electrical charge, if the molecular size of protein is not altered. Enhanced adsorption of a cationic derivative to the surface of the tissue would result in its increased permeability through the barrier. These findings provide useful information about the intestinal absorption of proteins of immunological and/or pharmacological importance in normal, healthy subjects.

This work is supported, in part, by a grant-in-aid for Scientific Research from the Ministry of Education, Culture, Sports, Science and Technology, Japan.

REFERENCES

1. **Ashwell G and Harford J.** Carbohydrate-specific receptors of the liver. *Annu Rev Biochem* 51: 531–554, 1982.
2. **Beglinger C, Born W, Muff R, Drewe J, Dreyfuss JL, Bock A, Mackay M, and Fischer JA.** Intracolonic bioavailability of human calcitonin in man. *Eur J Clin Pharmacol* 43: 527–531, 1992.
3. **Bickel U, Yoshikawa T, and Pardridge WM.** Delivery of peptides and proteins through the blood-brain barrier. *Adv Drug Delivery Rev* 46: 247–279, 2001.
4. **Blau S, Jubeh TT, Haupt SM, and Rubinstein A.** Drug targeting by surface cationization. *Crit Rev Ther Drug Carrier Syst* 17: 425–465, 2000.
5. **Castell JV, Friedrich G, Kuhn CS, and Poppe GE.** Intestinal absorption of undegraded proteins in men: presence of bromelain in plasma after oral intake. *Am J Physiol Gastrointest Liver Physiol* 273: G139–G146, 1997.
6. **Donovan MD, Flynn GL, and Amidon GL.** Absorption of polyethylene glycols 600 through 2000: the molecular weight dependence of gastrointestinal and nasal absorption. *Pharm Res* 7: 863–868, 1990.
7. **Dvorak AM.** Human basophil recovery from secretion. A review emphasizing the distribution of charcot-leyden crystal protein in cells stained with the postfixation electron-dense tracer, cationized ferritin. *Histol Histopathol* 11: 711–728, 1996.
8. **Felgner PL, Gadek TR, Holm M, Roman R, Chan HW, Wenz M, Northrop JP, Ringold GM, and Danielsen M.** Lipofection: a highly efficient, lipid-mediated DNA-transfection procedure. *Proc Natl Acad Sci USA* 84: 7413–7417, 1987.
9. **Franano FN, Edwards WB, Welch MJ, and Duncan JR.** Metabolism of receptor targeted ^{111}In-DTPA-glycoproteins: identification of ^{111}In-DTPA-epsilon-lysine as the primary metabolic and excretory product. *Nucl Med Biol* 21: 1023–1034, 1994.
10. **Gonnella PA and Neutra MR.** Membrane-bound and fluid-phase macromolecules enter separate prelysosomal compartments in absorptive cells of suckling rat ileum. *J Cell Biol* 99: 909–917, 1984.
11. **Habeeb AF.** Determination of free amino groups in proteins by trinitrobenzenesulfonic acid. *Anal Biochem* 14: 328–336, 1966.
12. **Haga M, Saito K, Shimaya T, Maezawa Y, Kato Y, and Kim SW.** Hypoglycemic effect of intestinally administered monosaccharide-modified insulin derivatives in rats. *Chem Pharm Bull (Tokyo)* 38: 1983–1986, 1990.

13. **Halpern SE.** The advantages and limits of indium-111 labeling of antibodies. Experimental studies and clinical applications. *Int J Rad Appl Instrum B* 13: 195–201, 1986.
14. **Hashida M, Nishikawa M, and Takakura Y.** Hepatic targeting of drugs and proteins by chemical modification. *J Controlled Release* 36: 99–107, 1995.
15. **He YL, Murby S, Warhurst G, Gifford L, Walker D, Ayrton J, Eastmond R, and Rowland M.** Species differences in size discrimination in the paracellular pathway reflected by oral bioavailability of poly(ethylene glycol) and D-peptides. *J Pharm Sci* 87: 626–633, 1998.
16. **Hnatowich DJ, Layne WW, and Childs RL.** The preparation and labeling of DTPA-coupled albumin. *Int J Appl Radiat Isot* 33: 327–332, 1982.
17. **Husby S, Jensenius JC, and Svehag SE.** Passage of undegraded dietary antigen into the blood of healthy adults. Quantification, estimation of size distribution, and relation of uptake to levels of specific antibodies. *Scand J Immunol* 22: 83–92, 1985.
18. **Hysing J, Tolleshaug H, and Curthoys NP.** Reabsorption and intracellular transport of cytochrome *c* and lysozyme in rat kidney. *Acta Physiol Scand* 140: 419–427, 1990.
19. **Kim DC, Harrison AW, Ruwart MJ, Wilkinson KF, Fisher JF, Hidalgo IJ, and Borchardt RT.** Evaluation of the bile acid transporter in enhancing intestinal permeability to renin-inhibitory peptides. *J Drug Target* 1: 347–359, 1993.
20. **Kiwada H, Morita K, Hayashi M, Awazu S, and Hanano M.** A new numerical calculation method for deconvolution in linear compartment analysis of pharmacokinetics. *Chem Pharm Bull (Tokyo)* 25: 1312–1318, 1977.
21. **Kohen R, Kakunda A, and Rubinstein A.** The role of cationized catalase and cationized glucose oxidase in mucosal oxidative damage induced in the rat jejunum. *J Biol Chem* 267: 21349–21354, 1992.
22. **Koizumi T, Arita T, and Kakemi K.** Absorption and excretion of drugs. XX. Some pharmacokinetic aspects of absorption and excretion of sulfonamides (2). Absorption from rat small intestine. *Chem Pharm Bull (Tokyo)* 12: 421–427, 1964.
23. **Koyama Y, Miyagawa T, Kawaide A, and Kataoka K.** Receptor-mediated absorption of high molecular weight dextrans from intestinal tract. *J Controlled Release* 41: 171–176, 1996.
24. **Lee YC, Stowell CP, and Krantz MJ.** 2-Imino-2-methoxyethyl 1-thioglycosides: new reagents for attaching sugars to proteins. *Biochemistry* 15: 3956–3963, 1976.
25. **Lovegrove JA, Osman DL, Morgan JB, and Hampton SM.** Transfer of cow's milk β-lactoglobulin to human serum after a milk load: a pilot study. *Gut* 34: 203–207, 1993.
26. **Mihara K, Hojo T, Fujikawa M, Takakura Y, Sezaki H, and Hashida M.** Disposition characteristics of protein drugs in the perfused rat kidney. *Pharm Res* 10: 823–827, 1993.
27. **Mihara K, Oka Y, Sawai K, Takakura Y, and Hashida M.** Improvement of therapeutic effect of human recombinant superoxide dismutase on is che mic acute renal failure in the rat via cationization and conjugation with polyethylene glycol. *J Drug Target* 2: 317–321, 1994.
28. **Mihara K, Sawai K, Takakura Y, and Hashida M.** Manipulation of renal disposition of human recombinant superoxide dismutase by chemical modification. *Biol Pharm Bull* 17: 296–301, 1994.
29. **Mizuma T, Ohta K, Koyanagi A, and Awazu S.** Improvement of intestinal absorption of leucine enkephalin by sugar coupling and peptidase inhibitors. *J Pharm Sci* 85: 854–857, 1996.
30. **Mizuma T, Sakai N, and Awazu S.** Na(+)-dependent transport of aminopeptidase-resistant sugar-coupled tripeptides in rat intestine. *Biochem Biophys Res Commun* 203: 1412–1416, 1994.
31. **Monsigny M, Roche AC, and Midoux P.** Uptake of neoglycoproteins via membrane lectin(s) of L1210 cells evidenced by quantitative flow cytofluorometry and drug targeting. *Biol Cell* 51: 187–196, 1984.
32. **Nishida K, Mihara K, Takino T, Nakane S, Takakura Y, Hashida M, and Sezaki H.** Hepatic disposition characteristics of electrically charged macromolecules in rat in vivo and in the perfused liver. *Pharm Res* 8: 437–444, 1991.
33. **Nishikawa M and Huang L.** Nonviral vectors in the new millennium: delivery barriers in gene transfer. *Hum Gene Ther* 12: 861–870, 2001.
34. **Nishikawa M, Ohtsubo Y, Ohno J, Fujita T, Koyama Y, Takakura Y, Hashida M, and Sezaki H.** Pharmacokinetics of receptor-mediated hepatic uptake of glycosylated albumin in mice. *Int J Pharm* 85: 75–85, 1992.
35. **Nishikawa M, Takakura Y, and Hashida M.** Pharmacokinetic evaluation of polymeric carriers. *Adv Drug Delivery Rev* 21: 135–155, 1996.
36. **Nishikawa M, Staud F, Takemura S, Takakura Y, and Hashida M.** Pharmacokinetic evaluation of biodistribution data obtained with radiolabeled proteins in mice. *Biol Pharm Bull* 22: 214–218, 1999.
37. **Pantzar N, Lundin S, Wester L, and Weström BR.** Bidirectional small-intestinal permeability in the rat to some common marker molecules in vitro. *Scand J Gastroenterol* 29: 703–709, 1994.
38. **Pape HC, Dwenger A, Regel G, Auf'm'Kolck M, Gollub F, Wisner D, Sturm JA, and Tscherne H.** Increased gut permeability after multiple trauma. *Br J Surg* 81: 850–852, 1994.
39. **Rescigno A and Segre G.** *Drug and Tracer Kinetics.* Waltham, MA: Blaisdell, 1966, p. 75–137.
40. **Rubinstein A, Kakunda A, and Kohen R.** Protection of the rat jejunal mucosa against oxidative injury by cationized superoxide dismutase. *J Pharm Sci* 82: 1285–1287, 1993.
41. **Saffran M, Field JB, Pena J, Jones RH, and Okuda Y.** Oral insulin in diabetic dogs. *J Endocrinol* 131: 267–278, 1991.
42. **Sanderson IR and Walker WA.** Uptake and transport of macromolecules by the intestine: possible role in clinical disorders (an update). *Gastroenterology* 104: 622–639, 1993.
43. **Schalkwijk J, van den Berg WB, van de Putte LB, Joosten LA, and van den Bersselaar L.** Cationization of catalase, peroxidase, and superoxide dismutase. Effect of improved intraarticular retention on experimental arthritis in mice. *J Clin Invest* 76: 198–205, 1985.
44. **Seifert J and Sass W.** Intestinal absorption of macromolecules and small particles. *Dig Dis* 8: 169–178, 1990.
45. **Selsted ME and Martinez RJ.** Lysozyme: primary bactericidin in human plasma serum active against *Bacillus subtilis*. *Infect Immun* 20: 782–791, 1978.
46. **Sezaki H and Hashida M.** Macromolecule-drug conjugates in targeted cancer chemotherapy. *Crit Rev Ther Drug Carrier Syst* 1: 1–38, 1984.
47. **Söderholm JD, Peterson KH, Olaison G, Franzén LE, Weström B, Magnusson KE, and Sjödahl R.** Epithelial permeability to proteins in the noninflamed ileum of Crohn's disease? *Gastroenterology* 117: 65–72, 1999.
48. **Takagi T, Kitano M, Masuda S, Tokuda H, Takakura Y, and Hashida M.** Augmented inhibitory effect of superoxide dismutase on superoxide anion release from macrophages by direct cationization. *Biochim Biophys Acta* 1335: 91–98, 1997.
49. **Takakura Y, Fujita T, Hashida M, and Sezaki H.** Disposition characteristics of macromolecules in tumor-bearing mice. *Pharm Res* 7: 339–346, 1990.
50. **Takakura Y, Mahato RI, Nishikawa M, and Hashida M.** Control of pharmacokinetic profiles of drug-macromolecule conjugates. *Adv Drug Delivery Rev* 19: 377–399, 1996.
51. **Tokuda H, Masuda S, Takakura Y, Sezaki H, and Hashida M.** Specific uptake of succinylated proteins via a scavenger receptor-mediated mechanism in cultured brain microvessel endothelial cells. *Biochem Biophys Res Commun* 196: 18–24, 1993.
52. **Triguero D, Buciak JB, Yang J, and Pardridge WM.** Blood-brain barrier transport of cationized immunoglobulin G: enhanced delivery compared with native protein. *Proc Natl Acad Sci USA* 86: 4761–4765, 1989.
53. **Yuzuriha T, Katayama K, and Fujita T.** Absorption route of 131-I-labeled lysozyme in rats. *Chem Pharm Bull (Tokyo)* 21: 2807–2809, 1973.
54. **Yuzuriha T, Katayama K, and Fujita T.** Studies on biotransformation of lysozyme. I. Preparation of labeled lysozyme and its intestinal absorption. *Chem Pharm Bull (Tokyo)* 23: 1309–1314, 1975.

Targeting Efficiency of Galactosylated Liposomes to Hepatocytes *in Vivo*: Effect of Lipid Composition

Aki Murao,[1] Makiya Nishikawa,[1] Chittima Managit,[1] Joseph Wong,[2] Shigeru Kawakami,[1] Fumiyoshi Yamashita,[1] and Mitsuru Hashida[1,3]

Received August 15, 2002; accepted August 29, 2002

Purpose. To investigate the effects of the lipid composition of galactosylated liposomes on their targeted delivery to hepatocytes.
Methods. Several types of liposomes with a particle size of about 90 nm were prepared using distearoyl-L-phosphatidylcholine (DSPC), cholesterol (Chol) and cholesten-5-yloxy-N-(4-((1-imino-2-D-thiogalactosylethyl)amino)butyl)formamide (Gal-C4-Chol), and labeled with [^{3}H]cholesterol hexadecyl ether. Their tissue disposition was investigated in mice following intravenous injection. The binding and internalization characteristics were also studied in HepG2 cells.
Results. Compared with [^{3}H]DSPC/Chol (60:40) liposomes, [^{3}H]DSPC/Chol/Gal-C4-Chol (60:35:5) liposomes exhibit extensive hepatic uptake. Separation of the liver cells showed that galactosylated liposomes are preferentially taken up by hepatocytes, whereas those lacking Gal-C4-Chol distribute equally to hepatocytes and nonparenchymal cells (NPC). Increasing the molar ratio of DSPC to 90% resulted in enhanced NPC uptake of both liposomes, suggesting their uptake via a mechanism other than asialoglycoprotein receptors. DSPC/Chol/Gal-C4-Chol (60:35:5) and DSPC/Chol/Gal-C4-Chol (90:5:5) liposomes exhibited similar binding to the surface of HepG2 cells, but the former were taken up faster by the cells.
Conclusions. The recognition of galactosylated liposomes by the asialoglycoprotein receptors is dependent on the lipid composition. Cholesterol-rich galactosylated liposomes, exhibiting less non-specific interaction and greater receptor-mediated uptake, are better for targeting drugs to hepatocytes *in vivo*.

KEY WORDS: liposome; asialoglycoprotein receptor; hepatocytes; drug targeting; internalization.

INTRODUCTION

Drug carriers with specific ligands for the corresponding receptors on the cell surface are useful for targeted drug delivery. Among various ligands investigated so far, galactose has been shown to be a promising targeting ligand to hepatocytes (liver parenchymal cells) because the cells possess a large number of the asialoglycoprotein receptors that recognize the galactose units on the oligosaccharide chains of glycoproteins or on chemically galactosylated drug carriers (1). The receptor-ligand interaction is known to show a significant "cluster effect" in which a multivalent interaction results in extremely strong binding of ligand to the receptors (2). We have already demonstrated that the *in vivo* recognition of galactosylated macromolecules by asialoglycoprotein receptors correlates with the degree of galactose modification (3–5). A pharmacokinetic analysis of the tissue disposition patterns of galactosylated proteins in mice has clearly shown that the density of galactose units on the protein surface determines the affinity of galactosylated proteins for asialoglycoprotein receptor-mediated hepatic uptake (4). These results indicate that the drug targeting efficiency to hepatocytes using galactosylated macromolecular carriers is dependent on the degree of galactose modification.

Liposomes are another class of drug carriers that have several advantages such as ease of preparation and a large capacity for drug loading (6). In previous papers, we synthesized a galactosylated cholesterol derivative and formulated it into neutral or cationic liposomes to obtain the galactosylated counterparts (7–11). These galactosylated liposomes were able to effectively deliver prostaglandin E_1, probucol and plasmid DNA to hepatocytes *in vivo*, indicating that the galactose units on the liposome surface can increase the affinity of the liposome for asialoglycoprotein receptors on hepatocytes. To ensure hepatocyte-specific targeting of liposomes by galactosylation, however, properties other than galactose density should also be controlled, such as the size and electric charge. The recognition of liposomes by the mononuclear phagocyte system (MPS) is known to be dependent on its lipid composition (12,13), which is an important factor in determining the surface properties of liposomes. Therefore, the clearance of liposomes from the circulation *in vivo* is highly dependent on the lipid composition (14). The surface properties of liposomes, such as the rigidity of the membrane and co-existence of two or more phases, is determined by their composition, which might affect the clustering of galactose units incorporated into a liposome formulation.

To understand the effects of the lipid composition of galactosylated liposomes on their targeted delivery to hepatocytes *in vivo*, various liposomes with or without galactose units were prepared involving different lipid mixing ratios: distearoyl-L-phosphatidylcholine (DSPC), cholesterol (Chol) a and galactosylated cholesterol derivative, and cholesten-5-yloxy-N-(4-((1-imino-2-D-thiogalactosylethyl)amino)butyl)formamide (Gal-C4-Chol). The liposomes were adjusted to a size of about 90 nm in diameter and radiolabeled with [^{3}H]cholesteryl hexadecyl ether (CHE). The tissue disposition of each type of liposome was studied in mice after intravenous injection. The distribution of liposomes within the liver (i.e., to hepatocytes or liver nonparenchymal cells (NPC)), was examined after digestion of the liver by collagenase. In addition, the internalization of liposomes was investigated in HepG2 cells *in vitro*. We report here that the lipid composition of the galactosylated liposomes is important for their recognition by asialoglycoprotein receptors.

[1] Department of Drug Delivery Research, Graduate School of Pharmaceutical Sciences, Kyoto University, Sakyo-ku, Kyoto 606-8501, Japan.
[2] I.V. Systems Division, Baxter Healthcare Corporation, Round Lake, Illinois 60073.
[3] To whom correspondence should be addressed. (e-mail: hashidam@pharm.kyoto-u.ac.jp)

ABBREVIATIONS: DSPC, distearoyl-L-phosphatidylcholine; Chol, cholesterol; Gal-C4-Chol, cholesten-5-yloxy-N-(4-((1-imino-2-D-thiogalactosylethyl)amino)butyl)formamide; NPC, nonparenchymal cells; MPS, mononuclear phagocyte system; CHE, cholesteryl hexadecyl ether; IME-thiogalactoside, 2-imino-2-methoxyethyl-1-thiogalactoside; Gal-BSA, galactosylated bovine serum albumin; HEPES, N-2-hydroxyethylpiperazine-N'-2-ethanesulfonic acid; CL_{liver}, liver uptake clearance; PC, phospholipid.

0724-8741/02/1200-1808/0 © 2002 Plenum Publishing Corporation

MATERIALS AND METHODS

Chemicals

N-(4-aminobutyl)carbamic acid *tert*-butyl ester was purchased from Tokyo Chemical Industry (Tokyo, Japan). DSPC and cholesteryl chloroformate was purchased from Sigma Chemical Co., (St. Louis, MO). Chol and Clear-Sol I were obtained from Nacalai Tesque (Kyoto, Japan), and Soluene 350 was purchased from Packard (Groningen, Netherlands). [^{3}H]CHE was purchased from NEN Life Science Products, Inc. (Boston, MA). 2-imino-2-methoxyethyl-1-thiogalactoside (IME-thiogalactoside) and galactosylated bovine serum albumin (Gal-BSA) were synthesized as reported previously (7). All other chemicals were of the highest purity commercially available.

Synthesis of Gal-C4-Chol

Gal-C4-Chol was prepared as reported previously (7). Briefly, cholesteryl chloroformate and N-(4-aminobutyl)carbamic acid *tert*-butyl ester were reacted in chloroform for 24 h at room temperature. A solution of trifluoroacetic acid and chloroform was added dropwise and the mixture was stirred for 4 h at 4°C. The solvent was evaporated to obtain N-(4-aminobutyl)-(cholesten-5-yloxyl)formamide then combined with IME-thiogalactoside and this mixture was then stirred for 24 h at room temperature. After evaporation, the resultant material was suspended in water, dialyzed against distilled water for 48 h (12 kDa cut-off dialysis tubing), then lyophilized.

Preparation of Liposomes

A mixture of DSPC and Chol, with or without Gal-C4-Chol, was dissolved in chloroform and evaporated to dryness in a round-bottomed flask. Then, the lipid film formed was resuspended in 5 ml sterile phosphate-buffered saline (pH 7.4). After hydration, the dispersion was sonicated for 5–10 min in a bath sonicator to form liposomes. Each suspension was extruded through a 100 nm pore size polycarbonate membrane at 60°C using an extruder (Northern Lipids, Vancouver, Canada). The concentration of Chol in each formulation was measured with a cholesterol E-test Wako kit (Wako Pure Chemicals, Osaka, Japan) and the lipid concentration was adjusted to 5 mg/ml.

The particle size of the liposomes was measured in a dynamic light scattering spectrophotometer (LS-900, Otsuka Electronics, Osaka, Japan). Radiolabeling of the liposomes was performed by addition of [^{3}H]CHE to the lipid mixture before formation of a thin film layer.

Tissue Disposition Study

All animal experiments were carried out in accordance with the Principles of Laboratory Animal Care as adopted and promulgated by the US National Institutes of Health and the Guidelines for Animal Experiments of Kyoto University. Five-week-old male ddY mice (25–27 g body weight) were obtained from Shizuoka Agricultural Co-operative Association for Laboratory Animals (Shizuoka, Japan). [^{3}H]liposomes at a dose of 25 mg/kg and 60 kBq/kg were injected into a tail vein. At predetermined time points, the mice were killed, and blood and urine were collected. The liver, kidney, spleen, heart, and lung were collected, washed with saline, blotted dry, and weighed. Ten microliters blood, 200 μl urine, and a piece of each tissue were digested with 0.7 ml Soluene-350 by incubating overnight at 45°C. Then, isopropanol (200 μl), 30% hydroperoxide (200 μl), 5 M HCl (100 μl) and, finally, Clear-Sol I (5 ml) were added. The samples were stored overnight and the radioactivity was measured using a scintillation counter (LSA-500, Beckman, Tokyo, Japan).

In different sets of experiments, 20 mg/kg Gal-BSA or 250 mg/kg DSPC/Chol liposome was first injected into mice. Then [^{3}H]DSPC/Chol/Gal-C4-Chol liposome at a dose of 25 mg/kg and 60 kBq/kg was injected and the liver was excised after 5 min.

Calculation of Clearance

Tissue distribution data were evaluated using organ clearances as reported previously (15). Briefly, the tissue uptake rate can be described by the following equation

$$\frac{dX_t}{dt} = CL_{uptake} C_b \tag{1}$$

where X_t is the amount of [^{3}H]liposomes in a tissue at time t, CL_{uptake} is the tissue uptake clearance, and C_b is the blood concentration of [^{3}H]liposomes. Integration of Eq. (1) gives

$$X_t = CL_{uptake} AUC_{0-t} \tag{2}$$

where AUC_{0-t} represents the area under the blood concentration-time curve from time 0 to t. Eq. (2) divided by C_b gives

$$\frac{X_t}{C_b} = \frac{CL_{uptake} AUC_{0-t}}{C_b} \tag{3}$$

The CL_{uptake} can then be obtained from the initial slope of a plot of X_t/C_b vs. AUC_{0-t}/C_b.

Intrahepatic Disposition

Mice were anesthetized with an intraperitoneal injection of pentobarbital sodium (50 mg/kg) and injected intravenously with [^{3}H]liposomes (25 mg/kg and 300 kBq/kg). The body temperature of the mice was kept at around 37°C with a heat lamp during the experiment. At 30 min after administration, the liver was perfused first with Ca^{2+}, Mg^{2+}-free perfusion buffer (10 mM N-2-hydroxyethylpiperazine-N'-2-ethanesulfonic acid (HEPES), 137 mM NaCl, 5 mM KCl, 0.5 mM NaH_2PO_4, and 0.4 mM Na_2HPO_4, pH 7.2) for 10 min and then with a perfusion buffer supplemented with 5 mM $CaCl_2$ and 0.05% (w/v) collagenase (type I) (pH 7.5) for 10 min. As soon as the perfusion started, the vena cava and aorta were cut and the perfusion rate was maintained at 3–4 ml/min. At the end of the perfusion, the liver was excised and its capsular membranes were removed. The cells were dispersed in ice-cold Hank's-HEPES buffer containing 0.1% BSA by gentle stirring. The dispersed cells were filtered through a cotton mesh sieve, followed by centrifugation at 50 × g for 1 min. The pellets containing hepatocytes were washed twice with Hank's-HEPES buffer by centrifuging at 50 × g for 1 min. The supernatant containing NPC was similarly centrifuged at least twice. The resulting supernatant was then centrifuged twice at 200 × g for 2 min. Hepatocytes and NPC were resuspended separately in ice-cold Hank's-HEPES buffer (4 ml for hepatocytes and 1.8 ml for NPC). The cell number and viability